Title
Improving the Lateral-Flow Immunoassay Using Aqueous Two-Phase Systems

Author
Le, Alexander Minh-Quan

Publication Date
2012

Peer reviewed|Thesis/dissertation

UNIVERSITY OF CALIFORNIA

Los Angeles

Improving the Lateral-Flow Immunoassay Using Aqueous Two-Phase Systems

A thesis submitted in partial satisfaction

of the requirements for the degree Master of Science

in Biomedical Engineering

By

Alexander Minh-Quan Le

2012

ABSTRACT OF THE THESIS

Improving the Lateral-Flow Immunoassay Using Aqueous Two-Phase Systems

By

Alexander Minh-Quan Le

Master of Science in Biomedical Engineering

University of California, Los Angeles, 2012

Professor Daniel T. Kamei, Chair

The objective of this thesis was to investigate a concentration method using aqueous two-phase systems (ATPS) for improving the detection of proteins and viruses at the point-of-care. In the first part of the thesis, aqueous two-phase micellar systems were generated using Triton X-114 surfactant to concentrate a model protein, namely transferrin (Tf). In the second part of the thesis, aqueous two-phase polymer-salt systems were generated using polyethylene glycol (PEG) and potassium phosphate salt to concentrate a model virus, namely bacteriophage M13 (M13). In both studies, the concentration step was combined with a detection assay, namely the lateral-flow immunoassay (LFA), to enhance the detection of protein and viral targets.

The detection of proteins at the point-of-need has several applications such as detecting food allergens in a food sample and protein toxins used as biowarfare agents in-field. For such applications, a sensitive, yet rapid, inexpensive, and portable detection assay that requires

minimal training and power is desired. Due to its ease of use, rapid processing, and minimal power and laboratory equipment requirements, the LFA is an appropriate assay for such applications. However, the LFA detection limit for proteins is inferior to lab-based assays, such as the enzyme-linked immunosorbent assay (ELISA), and needs to be improved. Aiming to improve the protein sensitivity of the LFA, we employed an aqueous two-phase micellar system composed of Triton X-114 surfactant to concentrate Tf prior to the detection step. However, one challenge with concentrating small biomolecules, such as proteins, is that they partition evenly between the two phases due to experiencing fewer excluded-volume interactions compared to larger biomolecules. To address this issue, we developed a novel approach involving larger colloidal gold nanoparticles decorated with anti-Tf antibodies in the concentration step to bind Tf and aid its transport to the micelle-poor phase. By manipulating the volume ratio of the two coexisting micellar phases to achieve higher concentrations, the Tf detection limit of LFA was improved by 10-fold from 0.5 μg/mL to 0.05 μg/mL. The ability to concentrate colloidal gold nanoparticles bound to Tf has opened up a whole new approach for improving the detection of smaller analytes with the LFA.

Viral detection in the point-of-care setting also has several applications. For example, the detection of infectious viral agents and pandemic pathogens, such as the swine-origin influenza A (H1N1) virus, is crucial for isolating confirmed cases and preventing outbreaks. The portability, simple operation procedure, rapid time to result, and minimal power and laboratory equipment requirements of the LFA make it an appropriate detection assay for such diagnostic applications. However, the viral sensitivity of the LFA is inferior to laboratory-based methods, such as viral culture and reverse-transcriptase polymerase chain reaction (PCR). We previously showed in a proof-of-principle study that the viral detection limit of the LFA could be improved

by concentrating a model virus, namely bacteriophage M13, using an aqueous two-phase micellar system prior to the detection step. The previous investigation represented the first time these two established technologies were ever combined. However, the micellar system exhibited slow phase separation times that were on the order of hours, indicating a need to improve the speed of the concentration step. Therefore, in this study, we investigated an aqueous two-phase polymer-salt system composed of polyethylene glycol (PEG) and potassium phosphate salt, which phase separates on the order of minutes, to concentrate M13. Furthermore, the colloidal gold nanoparticles used as the colorimetric indicator in the LFA were modified with a coated layer of PEG in order to improve their stability in the high salt content of the PEG-salt system. When M13 was concentrated using the PEG-salt system and combined with the LFA, the detection limit was improved by 10-fold from $5x10^8$ plaque forming units (pfu)/mL to $5x10^7$ pfu/mL. This study represents the first time that viral detection by LFA has been combined with a concentration method using an aqueous two-phase polymer-salt system. The faster phase separating ability of the PEG-salt system is a significant advance for applying this concentration method to improving point-of-care detection. Furthermore, the viable function of the modified colloidal gold nanoparticles coated with PEG in the LFA demonstrates a novel method for detecting biomolecules in ATPS containing high levels of salt.

The thesis of Alexander Minh-Quan Le is approved.

Dino Di Carlo

Benjamin M. Wu

Daniel T. Kamei, Committee Chair

University of California, Los Angeles

2012

This is dedicated to my mother, Huyen

Table of Contents

List of Figures

List of Tables

Acknowledgments

This work would not have been possible without the support and guidance from all those around me. First and foremost, I would like to thank my advisor and mentor, Dr. Daniel T. Kamei for his wholehearted guidance and support. Over the past three years I have had the great opportunity to take all his undergraduate and graduate classes and to work under his guidance as both an undergraduate and graduate researcher. It has all been such a wonderful and phenomenal experience. I have developed so much, and I owe much of what I have gained to him. Dan has always been so caring, and he always inspires me to strive for excellence and to be the best that I can be. He is the perfect role model as his unwavering work ethic, determination, honesty, compassion, and attention to detail are such admirable attributes that I look up to. He has taught me so many life lessons that I am happy to take away. I have learned so much from you Dan, and I appreciate it very much. I thank you with my whole heart.

I would also like to thank Dr. Foad Mashayekhi, my graduate student mentor, who I've had the chance to start working on my first research project with. Working with Foad over the past three years he has given me such a strong foundation with his guidance since the beginning of my development as a researcher. I thank him for always keeping me on track. I am happy to have seen Foad go through the process of developing the technology to start his own company, and it has been a very rewarding experience. Ricky Chiu has also been a great help with his knowledge of the LFA technologies. He has helped me troubleshoot the LFA test many times.

I would also like to thank the other members of the Kamei Lab who I have had the chance to work alongside with over the years. Stacey Shiigi and Aaron Meyer, who were my senior mentors, trained me when I first began research. Felix Chao helped me with the M13 partitioning experiments that led to my first ever scientific article publication. Together with my

LFA partner, Parsa Nafisi, we have constructed a countless number LFA membranes. Parsa has always been a great help with the partitioning and LFA experiments. During one of his summers, Parsa made a great advance in developing the method for modifying the colloidal gold nanoparticles with PEG, which was ultimately used for our PEG-salt concentration experiments. Cameron Yamanishi has been a great help with his M13 concentration experiments in the PEG-salt system. Our Giants-Dodger rivalry will always live on. I would like thank the rest of all my friends in the Kamei Lab who have made my UCLA experience especially spectacular. I will always remember all the fun we've had and our special bonds with each other.

Last of all, I would like to thank my all of my family, for supporting me all throughout my time here at UCLA, especially my mother, Huyen, whom I admire so much for her resiliency, strength, and for always being there for me. To my cousins, aunts, and uncles, thank you for always mentioning how proud you all are of me and for treating me with such great food when I visited home.

Chapter 2 is a version of: F. Mashayekhi, R.Y.T. Chiu, A. Le, F. Chao, B. Wu, and D.T. Kamei, *Enhancing the lateral-flow immunoassay for viral detection using an aqueous two-phase micellar system*. Anal Bioanal Chem, 2010. 398(7): 2955-2961, Springer Copyright © 2010. Reprinted with permission of Springer. D.T. Kamei was the director of research for this article. This work was supported by UCLA funds to D.T. Kamei.

Chapter 1: Introduction

1.1. Motivation and Background

The focus of this thesis was to investigate a method to improve the sensitivity of a biomolecule detection assay, namely the lateral-flow immunoassay (LFA), for the detection of two biomolecule targets: proteins and viruses. Our approach employed the use of aqueous two-phase systems (ATPS) to concentrate a model protein, namely transferrin (Tf), and a model virus, namely bacteriophage M13 (M13), prior to their detection via LFA. This chapter summarizes the motivation for investigating the detection of proteins and viruses, and also describes the aqueous two-phase systems employed along with the LFA technologies.

1.1.1. Protein Detection

The detection of proteins has a variety of applications, such as detecting food-allergens at the point-of-need or defending against protein toxins used as biological warfare agents. In the case of food allergens, under the Food Allergen Labeling and Consumer Protection Act (FALCPA) in the US, food manufacturers must indicate whether pre-identified food allergens are used as ingredients [1]. However, this labeling does not account for food allergens present in products due to contamination during transportation or the production process [2]. Therefore, a sensitive, yet rapid and inexpensive assay, which could be used at the point-of-need, may result in more frequent screening of food products by the manufacturers, benefitting both food manufactures and consumers. Furthermore, protein detection would also prove useful in defending against bioterrorism agents. For example, protein toxins used in biological warfare, such as ricin toxin, are typically invisible to the naked eye, odorless, tasteless, and may not cause an immediate reaction [3-4]. In order to minimize their spread and harmful impact to the civilian

population, it is essential to provide the authorities with the means to rapidly detect bioterrorism agents in-field at the point-of-need.

For detecting proteins at the point-of-need, one detection method that has gained much attention in recent years due to its ease of use, rapid time to result, and minimal power and laboratory equipment requirements is the LFA. The LFA utilizes a test strip that collects a sample through lateral-flow, and detects the presence of a target molecule through its specific antibody labeled with a colorimetric indicator, such as colloidal gold nanoparticles [5]. The LFA has previously been used for the detection of protein targets [6-8]. Compared to lab-based assays, such as the enzyme-linked immunosorbent assay (ELISA), the LFA does not require laboratory equipment and provides a faster time to result (Table 1.1). However, the detection limit of LFA for proteins, such as food allergens, is still inferior to the ELISA (Table 1.2) and needs to be improved [8-9].

Table 1.1. Comparison of the required equipment and time to result of various protein detection methods.

Detection method	Required equipment	Time
ELISA	ELISA plate reader	30-60 min [8]
LFA	No laboratory equipment	< 10 min [8]

Table 1.2. Comparison of LFA and ELISA detection limits for various food allergens.

Food allergen	LFA detection limit (ppm)	ELISA detection limit (ppm)
Cereals with gluten	10	2.50
Crustaceans	5	0.05
Peanuts	1	0.15
Milk	<5	0.12
Almond	1	0.17
Hazelnut	1	0.15

Furthermore, the allergic threshold concentration levels of some food allergens are too low to be detected by LFA, such as the peanut allergen. Previous studies have determined the

threshold of allergic reaction, or No Observed Adverse Effect Level (NOAEL), of peanut allergens to be approximately 30 µg [10]. However, in order to detect this threshold level in food serving sizes, which are typically greater than 250 g for meals [11], this would require a detection limit lower than 0.12 µg of peanut allergen out of 1 g of food. According to Table 1.2, the LFA detection limit for peanut allergen is 1 ppm, or 1 µg of peanut allergen out of 1 g of food. Therefore, this demonstrates that there is a need to improve the sensitivity of the LFA.

1.1.2. Viral Detection

The detection of viral agents also has many useful applications. The outbreak of swine-origin influenza A (H1N1) virus infection [12] highlighted the need for a means to rapidly and accurately diagnose and detect infectious agents and pandemic pathogens at the point-of-care. Rapid and accurate diagnosis of such agents and pathogens at the point-of-care would result in better patient management, such as timely use of appropriate antiviral treatments, isolation of confirmed cases, and prevention of outbreaks [13-14]. Furthermore, viral detection can be utilized to defend against biowarfare agents, such as Ebola or Marburg viruses. Frontline military personnel would benefit from a point-of-care viral detection device that would allow protection from such harmful viral biowarfare agents.

For the detection of viruses at the point-of-care, the LFA can be an appropriate detection assay. As mentioned previously, the LFA requires minimal laboratory equipment, provides fast time to result, and is portable. However, while the LFA has been used to detect a wide range of biomolecules [15-22], its sensitivity has been shown to be inferior to the gold standards for viral detection, namely viral culture and real-time or reverse-transcriptase polymerase chain reaction (PCR) [14, 18, 23-27]. For example, LFA sensitivity and specificity has been shown to range

between 19% to 32%, and 96% to 99.6%, respectively, when the LFA test (QuickVue Influenza A+B Test, Quidel, San Diego, CA) was compared to reverse-transcriptase PCR [14]. In another study, the sensitivity of the QuickVue Influenza A+B Test was found to be 51%, 63%, and 31% for detecting swine-origin influenza virus, H1N1 seasonal influenza virus, and H3N2 influenza virus, respectively, when compared to reverse-transcriptase PCR [27]. Although LFA offers advantages over viral culture and PCR in terms of ease of use and rapid time to result (Table 1.3), its low sensitivity in detecting pathogens and viruses (Table 1.4) has rendered it an ineffective point-of-care detection assay for preventing pandemic outbreaks. Therefore, the need to improve the sensitivity of LFA for detection of infectious agents definitely exists.

Table 1.3. Comparison of the required equipment and time to result of various viral detection methods.

Detection method	Required equipment	Time
Viral culture	Incubator, centrifuge	1-14 days [28-29]
PCR	Thermal cycler, gel electrophoresis	4-6 hours [30]
LFA	No laboratory equipment	< 10 min [8]

Table 1.4. LFA sensitivity compared to PCR for detection of various viral targets

Viral target	LFA sensitivity compared to PCR
Influenza A and B	19-32% [14]
Swine-origin influenza virus	51% [27]
H1N1 seasonal influenza virus	63% [27]
H3N2 influenza virus	31% [27]

1.2. Aqueous Two-Phase Systems

In order to improve the sensitivity of the LFA for protein and viral particle targets, we investigated a method to concentrate the biomolecule targets prior to their detection. Since the concentration step is to be combined with a detection assay designed to be used at the point-of-care or in low-resource settings, small samples are typically preferred. Liquid-liquid extraction is one separation method that can be readily scalable for small sample sizes [31]. However, conventional oil-water systems cannot be used for separating biomolecules as such molecules tend to denature in nonpolar solvents. On the other hand, aqueous two-phase complex fluid systems are comprised primarily of water, and therefore, these solvents are less prone to denaturing biomolecules. The partitioning of cells, proteins, viruses, and nucleic acids in aqueous two-phase systems have been investigated for several years [32-51]. However, the main focus of these previous studies has been on large-scale purifications for the biotechnology and pharmaceutical industries. In this project, we instead examined this technology for small-scale diagnostic applications, such as the detection of food allergens, protein toxins, and infectious viral agents.

There are various types of aqueous two-phase systems (ATPS) that may be employed. For instance, ATPS may be comprised of (i) surfactant or (ii) polymer and salt constituents [34, 38, 52]. When such constituents are mixed together in an aqueous solution, and at appropriate operating temperatures and concentrations of the constituents, the solution can undergo a macroscopic phase separation [34]. Biomolecules have been found to partition, or distribute unevenly between the two distinct macroscopic phases depending on physico-chemical characteristics such as hydrophobicity [38, 53] and size [54-55]. Through manipulating the volume ratio between the two-macroscopic phases, higher concentrations of a target biomolecule

can be achieved. In this study, two types of ATPS were used to concentrate proteins and viruses. In the first part of the study, aqueous two-phase micellar systems were used to concentrate a model protein, namely transferrin. In the second part of the study, aqueous two-phase polymer-salt systems were used to concentrate a model virus, namely bacteriophage M13. The following sections describe these ATPS in further detail.

1.2.1. Aqueous Two-Phase Micellar Systems

Aqueous two-phase micellar systems are primarily comprised of water and surfactant. Surfactants are amphiphilic molecules which, when placed in an aqueous environment, self-assemble into aggregates called micelles, when the surfactant concentration is above the critical micelle concentration (CMC). In the structure of a micelle, hydrophobic tails face inwards and hydrophilic heads face outwards [56-57]. Above a temperature known as its cloud point (specific to a particular surfactant concentration), an aqueous solution containing a nonionic surfactant can separate into two macroscopic phases, a micelle-rich phase and a micelle-poor phase.

In one of the studies, we used Triton X-114 surfactant to form the aqueous two-phase micellar system. At low temperatures, the Triton X-114 micellar system exhibits a homogeneous, isotropic phase. However, upon increasing the temperature, the solution undergoes a macroscopic phase separation to yield a top, micelle-poor phase and a bottom, micelle-rich phase as shown schematically in Figure 1.1 below. This phenomenon occurs since the increase in the thermal energy of molecules weakens the hydrogen bonds between water molecules and hydrophilic heads of the micelles. As a result, the micelle-water interactions become less favorable, and the micelle-micelle interactions become more favorable due to their ability to approach each other more closely and increase their van der Waals attractive interactions. This

allows the formation of micelle-poor and micelle-rich domains. These respective domains coalesce together and move up or down depending on their relative densities leading to the formation of two macroscopic phases.

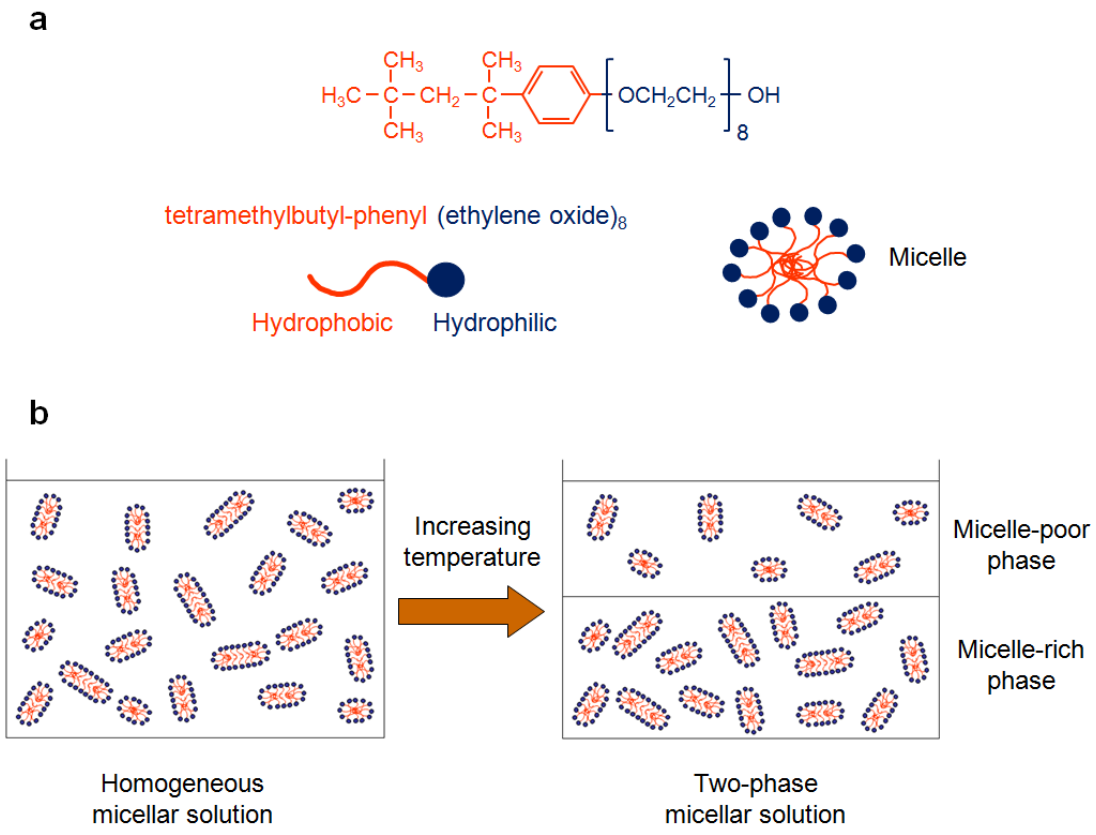

Figure 1.1. (a) Chemical structure of the Triton X-114 surfactant, and schematic representations of the Triton X-114 surfactant and micelle. (b) Schematic representation of the aqueous two-phase Triton X-114 micellar system phase separating upon an increase in temperature.

After phase separation, each phase can be extracted and analyzed for the presence of target biomolecules. Large hydrophilic macromolecules, such as genomic DNA fragments and viruses partition primarily into the top, micelle-poor phase due to the greater excluded-volume interactions that operate between the DNA fragment or virus and the larger number of micelles in the bottom, micelle-rich phase [58-59]. However, unlike viruses and genomic DNA, smaller water-soluble proteins partition fairly evenly between the two phases of an ATPS [40, 43-44, 54,

60] as they do not experience as many excluded-volume interactions due to their smaller size. This in turn would result in limited concentration of such proteins into one of the two phases. To overcome this shortcoming associated with proteins, our research group has developed a novel approach to "fish" the target protein into the top micelle-poor phase using large hydrophilic colloidal gold nanoparticles (see Chapter 2). The volume ratio can then be manipulated to achieve higher concentrations of the target protein through altering operating conditions such as temperature and surfactant concentration.

1.2.2. Aqueous Two-Phase Polymer-Salt Systems

There also exist aqueous two-phase systems that can form when a specific polymer and specific salt is added together in an aqueous solution. One such example is an aqueous solution containing polyethylene glycol (PEG) and potassium phosphate salt. At low concentrations of polymer and salt, the aqueous solution exists as a single homogeneous phase. When the concentration of salt is increased, phase separation occurs. One explanation for this phase separation phenomenon is similar to the one mentioned earlier for the surfactant systems. Specifically, the salt ions dehydrate the ethylene oxide units of PEG, which make the PEG-water interactions less favorable and the PEG-PEG interactions more favorable. Another hypothesis is that the addition of certain salts creates two different water structure types that are incompatible with each other leading to the formation of two immiscible phases [61-62]. Specifically in PEG-salt systems, the PEG polymer contains an ether oxygen whose dipole can interact with salt cations. However, experimental evidence has shown that some cations, particularly those with small multivalent anions of high charge density, are unable to interact with the PEG ether oxygen dipoles perhaps due to the proximity of electron-donating groups on the PEG molecule [61].

Such types of salt ions consequently create a region of salt-depleted water around the polymer as they are unable to approach the PEG molecule. The water structure of the salt-poor regions around the polymer is different than the water structure of salt-rich regions. Due to the incompatibility between the polymer-rich, salt-poor regions and polymer-poor, salt-rich regions, the polymers coalesce together to maximize their number of possible configurations and to minimize their interaction with the salt-rich regions. This leads to the formation of polymer-rich, salt-poor and polymer-poor, salt-rich domains. The domains eventually coalesce together, and due to their density difference, move up or down accordingly. Once near equilibrium, two distinct macroscopic phases are formed in the solution: a top polymer-rich, salt-poor phase and a bottom polymer-poor, salt-rich phase [63].

Aqueous two-phase systems involving polymers have been previously utilized to concentrate and purify viruses from sewage water [64] as well as culture supernatant [65]. In this study, a polymer-salt ATPS using PEG and potassium phosphate salt was employed to concentrate M13. Macromolecules have been shown to partition in PEG-salt systems based on hydrophobicity [61] and size [66]. Hydrophilic biomolecules such as hydrophilic proteins partition more into the bottom polymer-poor, salt-rich phase of PEG-salt systems [61]. Due to the outer hydrophilic coat of M13 [67], the virus is expected to partition into the bottom polymer-poor, salt-rich phase. Furthermore, large linear polymers form a mesh network in solution limiting the size of the macromolecule that can be contained in the polymer-rich phase [66]. Thus, due to the excluded-volume interactions that operate between the viral particles and the polymer molecules in the top polymer-rich phase, viral partitioning is expected to be driven to the bottom polymer-poor, salt-rich phase. The volume ratio between the bottom, polymer-poor

phase and top, polymer-rich phase can also be manipulated to achieve higher concentrations of the target virus.

1.3. Lateral-Flow Immunoassay

Immunoassays are generally performed to detect molecules from human samples to identify certain diseases or conditions. Immunoassays have a broad range of applications as they can detect target molecules such as frequent drugs of abuse [20], hormones [21], toxins [22], and pathogens [15]. The lateral-flow immunoassay (LFA) utilizes a test strip that collects a sample through lateral flow, and detects the presence of a target molecule through its specific antibody bound to a colorimetric indicator, such as colloidal gold nanoparticles that exhibit a dark-red to purple color [68-69]. LFA requires minimal sample volumes, yields results rapidly, and requires minimal laboratory skills, making it an attractive option for a point-of-care detection device.

A traditional LFA test strip, shown schematically in Figure 1.2, consists of 4 main components: sample pad, nitrocellulose membrane, absorbent pad, and adhesive vinyl backing. The sample pad is located at the lower end of the test strip, where the test trip first makes contact with the solution. The solution then flows by capillary action up to the absorbance pad through the nitrocellulose membrane. The sample pad functions as a filter to block large debris or other particles, such as cells, that might be present in the sample. Detection occurs on the nitrocellulose membrane where antibodies are immobilized to capture the target molecule. The absorbent pad, located at the upper end of the test strip, acts as a sink to absorb excess liquid. The final component is the adhesive vinyl backing, which holds all the components together and provides physical support for the strip [70].

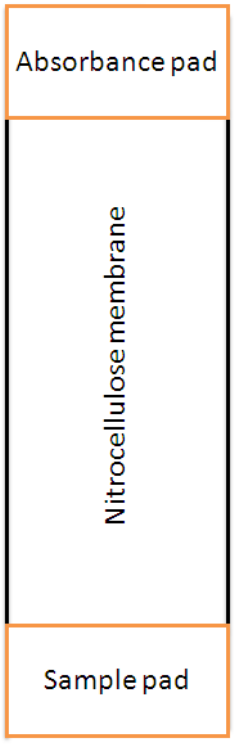

Figure 1.2. Schematic representation of an LFA strip. The adhesive vinyl backing, which lies underneath the sample pad, the nitrocellulose membrane, and the absorbance pad, does not appear in this schematic.

1.3.1. Competition Assay

There are two different approaches for the lateral-flow immunoassay: the sandwich assay and the competition assay. In the first part of this thesis, the competition assay was utilized for the detection of the transferrin protein. The schematic of the competition assay is shown below in Figure 1.3. In the competition LFA assay, the entire target of interest, or a portion of the target (such as a nontoxic chain of a toxin molecule), is immobilized on a nitrocellulose membrane in the form of a line, called the test line. The colloidal gold probes (AuP), which are used as the colorimetric indicator for the LFA, have primary antibodies specific for the target protein immobilized on the surface of the nanoparticle. Secondary antibodies specific to the primary antibody bound on these AuP are also immobilized on the nitrocellulose membrane in the form of a line, called the control line. In LFA, a sample first comes into contact with the AuP. If the

target molecules are present in the sample, they would first bind to their specific antibodies on the AuP. If the sample has enough target molecules to saturate the target-specific antibodies on the AuP, the target-specific antibodies in the AuP cannot bind to the immobilized target molecules on the test line, and hence do not form a visual band at the test line. This indicates a positive result as shown in Figure 1.3a. Alternatively, if the sample does not contain the target molecules at a concentration that saturates the target-specific antibodies immobilized on the colloidal gold nanoparticles, the target-specific antibodies on the AuP can bind to the immobilized target, and form a visual band at the test line indicating a negative result as shown in Figure 1.3b. Furthermore, regardless of the presence of the target molecule in the sample, AuP will bind to the immobilized secondary antibodies on the control line, indicating a valid test.

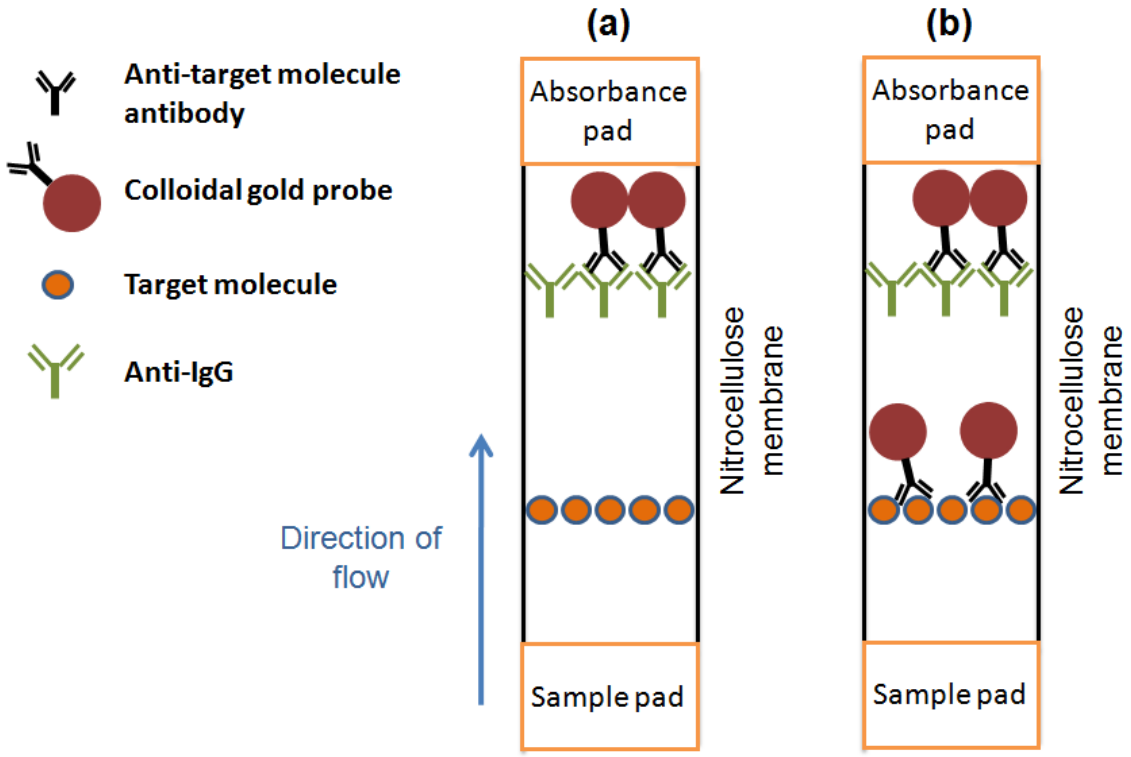

Figure 1.3. Schematic representation of (a) positive and (b) negative results for the LFA using the competition assay mechanism.

1.3.2. Sandwich Assay

In the second part of this thesis, the sandwich assay was utilized to detect the presence of M13. The schematic of the sandwich assay is shown in Figure 1.4. For this method, two different types of AuP were used, one designed to bind only to the test line and the other designed to bind only to the control line. The first AuP (AuP_{test}), which contains antibodies specific for the target biomolecule coated on its surface, is designed to bind only to the test line. The second AuP ($AuP_{control}$), which is coated with a different antibody that does not bind the target biomolecule, is designed to bind only to the control line. Antibodies specific for the target biomolecule are immobilized on a nitrocellulose membrane in a line, called the test line. Secondary antibodies specific for the primary antibody on $AuP_{control}$ are also immobilized on the nitrocellulose membrane above the test line, to form the control line. In LFA, a sample first comes into contact with the target-specific antibodies bound on AuP_{test}. If the target molecules are present in the sample, they will first bind to their specific antibodies on the AuP_{test}. As the AuP_{test}-target protein complexes move up the LFA strip, the targeted protein will bind to their specific antibodies immobilized on the test line. Due to trapping of the colloidal gold nanoparticles, which exhibit a purple red color, a visual band is formed at the test line indicating a positive result (Figure 1.4a). Alternatively, if the target molecule is not present in the solution, the colloidal gold probes will not bind to the immobilized antibodies at the test line, indicating a negative result (Figure 1.4b). Furthermore, regardless of the presence or lack of the target molecule in the sample, $AuP_{control}$ will bind to the immobilized secondary antibodies on the control line, indicating a valid test.

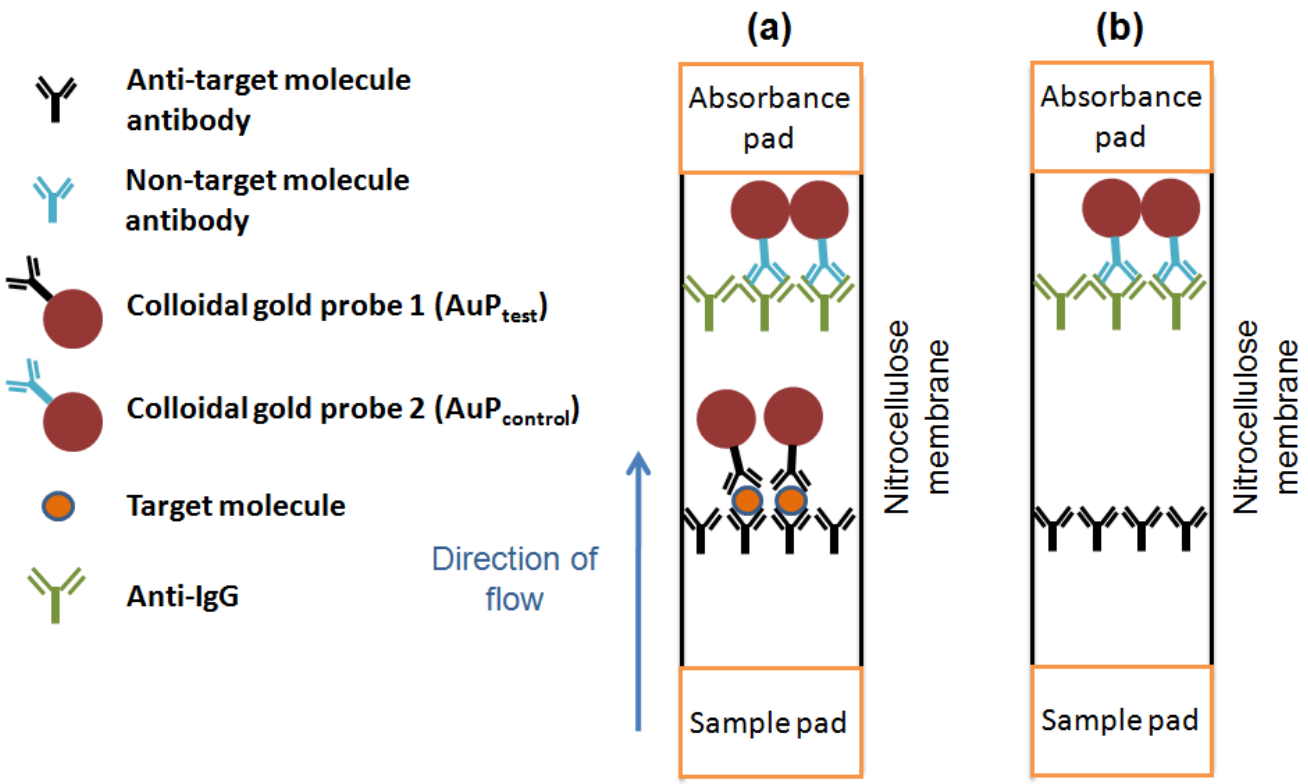

Figure 1.4. Schematic representation of (a) positive and (b) negative results for the LFA using the sandwich assay mechanism.

Chapter 2: Concentrating Transferrin Using an Aqueous Two-Phase Micellar System to Improve Detection with the Lateral-Flow Immunoassay

2.1. Introduction

Proteins are markers for a wide variety of applications, such as detecting food allergens and protein toxins. In the case of food allergens, under the Food Allergen Labeling and Consumer Protection Act (FALCPA) in the US, food manufacturers are required to indicate the presence of any of the 8 pre-identified food allergens only if they are used as ingredients [1]. However, this labeling does not account for food allergens present in products due to contamination caused by using shared transportation containers and production lines [2]. Therefore, a sensitive, yet rapid and inexpensive assay, which could be used at the point-of-need (PON), may lead to more frequent screening of food products by the manufacturers, and could be beneficial to both food manufactures and consumers.

In the case of protein toxins, bioterrorism agents (BAs), such as ricin toxin, present great danger to the general public, since they are usually invisible to the naked eye, odorless, tasteless, and may not cause an immediate reaction [3-4]. In order to minimize their spread and harmful impact to the civilian population, it is essential to provide the authorities with the means to rapidly detect BAs in-field and at the PON.

One detection method that has gained much attention in recent years due to its ease of use, rapid time to result, and minimal power and laboratory equipment requirements is the lateral-flow immunoassay (LFA). LFA utilizes a test strip that collects a sample through lateral flow, and detects the presence of a target molecule through its specific antibody labeled with a colorimetric indicator, such as colloidal gold nanoparticles. LFA has previously been used for the detection of protein targets [6-8]. However, the detection limit of LFA is still inferior to lab-

based assays, such as the enzyme-linked immunosorbent assay (ELISA), and needs to be improved [8-9].

One approach to achieve a higher sensitivity for LFA is to improve the assay itself. Another approach is to concentrate the target molecule prior to the detection step, and we have focused on this latter approach. However, for the detection assay to still be implementable at the PON, the concentration step must also be implementable at the PON, meaning it must be simple to perform and require minimal training and power. One method that meets these criteria is liquid-liquid extraction using aqueous two-phase systems (ATPS). ATPS, which can be formed with micelles (ATPMS), polymers (ATPPS), or a combination of the two, have generally been examined for large-scale biotechnological applications [34, 38-39, 43-44, 58, 71] and not small-scale diagnostic applications. We previously, and for the first time, combined the established technologies of LFA and ATPS to improve the detection limit of LFA in detecting a model virus [72]. This paper represents a follow-up to that work, where a proof-of-principle study for protein markers, was performed. Specifically, we investigated the concentration of human transferrin (Tf), our model protein, using an ATPMS prior to its detection via LFA. Tf transports iron in serum, and has a molecular weight of about 78 kDa. It was chosen as our model protein due to it being similar in size to some known allergens, and our research group's experience with its radiolabeling.

In this first part of the thesis, an ATPMS comprised of the nonionic surfactant Triton X-114 and phosphate-buffered saline (PBS) was investigated for concentrating Tf. In an aqueous solution at concentrations above their critical micelle concentration (CMC), the surfactant molecules form micelles [57]. The Triton X-114 micellar system exhibits a homogeneous, isotropic phase at low temperatures. However, upon increasing the temperature, the solution

undergoes a macroscopic phase separation to yield a top, micelle-poor phase and a bottom, micelle-rich phase. Biomolecules would then distribute, or partition, unevenly between the two phases based on their physico-chemical characteristics, such as hydrophobicity [53] and size [54].

Unlike large hydrophilic macromolecules, such as genomic DNA fragments and viruses [58-59], water-soluble proteins partition fairly evenly between the two phases of an ATPS [40, 43-44, 54, 60], which in turn would result in limited concentration of such proteins into one of the two phases. Accordingly, a novel approach was investigated to concentrate the target proteins into the top, micelle-poor phase. In this approach, as shown schematically in Figure 2.1, the target proteins are "fished" into the top, micelle-poor phase by utilizing hydrophilic, colloidal gold particles, which are nanometers in diameter, and are coated with antibodies specific for the target proteins. The colloidal gold-antibody-target protein complex is then expected to partition extremely into the top, micelle-poor phase based on the greater repulsive, steric, excluded-volume interactions that operate between the colloidal gold nanoparticles and micelles that are present in the bottom, micelle-rich phase. Therefore, similar to DNA and viral partitioning, if the target protein partitions extremely into the top, micelle-poor phase, it can be concentrated in that phase by reducing its volume relative to the bottom, micelle-rich phase. Furthermore, another advantage of this approach is that the concentrated colloidal gold-antibody-target protein complexes could directly be utilized in the subsequent downstream LFA detection step.

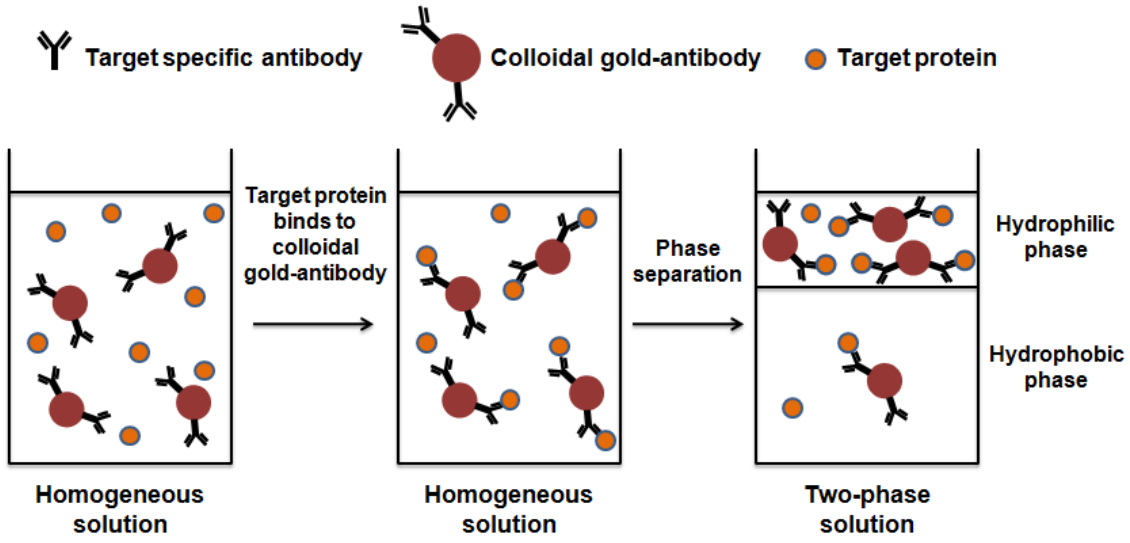

Figure 2.1. Schematic representation of the method for concentrating target proteins in an aqueous two-phase micellar system using colloidal gold nanoparticles that are decorated with target-specific antibodies. The y-shaped object, the red circle, and the orange circle represent the antibody, the colloidal gold nanoparticle, and the target molecule, respectively.

In this study, the partitioning behavior of the target protein was investigated with the system described above using Triton X-114 as the surfactant. Specifically, the partition coefficients of gold nanoparticles and Tf, with or without utilizing colloidal gold nanoparticles for enhancing Tf partitioning were measured. In addition, gold nanoparticles and Tf were concentrated in the top, micelle-poor phase by manipulating the volume ratio (the volume of the top, micelle-poor phase divided by that of the bottom, micelle-rich phase). Furthermore, we developed an LFA for the detection of Tf in-solution. Once the detection limit of the immunoassay was established, Tf was concentrated by utilizing the ATPMS prior to the detection step to investigate the effect of the concentration step on the detection limit of LFA.

2.2. Materials and Methods

2.2.1. Radiolabeling of Transferrin and Anti-Transferrin Antibody

Tyrosine residues of iron-loaded Tf and goat polyclonal anti-Tf antibody (Bethyl Laboratories, Montgomery, TX) were radiolabeled with $Na^{125}I$ (MP Biomedicals, Irvine, CA) using IODO-BEADS (Pierce Biotechnology, Rockford, IL). The radiolabeled proteins were purified from free iodine-125 using a Sephadex G10 size-exclusion column in the presence of bovine serum albumin (BSA) to inhibit nonspecific binding to the column. The phosphotungstic acid assay was used to quantify the specific activity and concentration of the radiolabeled proteins. All reagents and materials were purchased from Sigma-Aldrich (St. Louis, MO) unless otherwise noted.

2.2.2. Preparing Colloidal Gold Probes

The colloidal gold nanoparticles were prepared according to Frens [73]. Using this method, a solution of colloidal gold nanoparticles with an average hydrodynamic radius of 19 nm was obtained, which appeared as a clear, dark cherry-colored solution. The size of the colloidal gold nanoparticles was obtained by using a Zetasizer Nano ZS particle analyzer (Malvern Instruments Inc, Westborough, Massachusetts) following the manufacturer's instructions.

The colloidal gold-anti-Tf complexes, henceforth referred to as gold probes (AuP), were prepared as described by Horisberger and Clerc [74]. Briefly, the pH of a 2.5 mL colloidal gold nanoparticle solution was adjusted to pH 9 using 0.1 M NaOH. Subsequently, 40 µg of anti-Tf antibody at a concentration of 0.1 mg/mL was added to the colloidal gold solution and mixed for

1 hour on a shaker. To prevent nonspecific binding of other proteins to the surfaces of the colloidal gold nanoparticles, 250 µL of a 10% w/v BSA solution was added to the mixture and mixed for 15 min on a shaker. To remove free, unbound antibodies, the mixture was then centrifuged for 30 min at room temperature and 4000 g, followed by resuspending the pellet of colloidal gold nanoparticles in 1.3 mL of a 1% w/v BSA solution. The centrifugation and resuspension step was repeated two more times, and after the third centrifugation, the pellet of gold nanoparticles was resuspended in 375 µL of 0.1 M sodium borate buffer at pH 9.0. The average hydrodynamic radius of the AuP was also found by using the Zetasizer Nano ZS particle analyzer.

The above protocol was also carried out in triplicate with radiolabeled anti-Tf antibodies to quantify the amount of antibody bound to the gold nanoparticles. After each centrifugation step, the amount of free radiolabeled anti-Tf antibody in the supernatant was measured by using a Cobra Series Auto-Gamma Counter (Packard Instrument Co., Meriden, CT). After resuspending the gold nanoparticles for the third and final time in 0.1 M sodium borate buffer, the amount of radiolabeled anti-Tf antibodies bound to gold particles was measured by using the Cobra Series Auto-Gamma Counter.

2.2.3. Partitioning Colloidal Gold Probes

Colloidal gold nanoparticles bound to radiolabeled anti-Tf antibodies were partitioned in ATPMS. For each partitioning experiment, four identical 3.5 mL Triton X-114 solutions in Dulbecco's phosphate-buffered saline (PBS, Invitrogen, pH 7.4, containing 1.47 mM KH_2PO_4, 8.10 mM Na_2HPO_4, 138 mM NaCl, 2.67 mM KCl, and 0.495 mM $MgCl_2$) were prepared. 5 µL of colloidal gold nanoparticles bound to radiolabeled anti-Tf antibodies (radioactive AuP) were

added to three of the solutions. The fourth solution served as the control which did not contain any radioactive AuP. In order to ensure that each solution was in one phase prior to phase separation, the solutions were equilibrated at 4°C prior to the addition of the radioactive AuP. Once radioactive AuP were added, the solutions were mixed and placed in a water bath set at the appropriate temperature which yielded a volume ratio equal to approximately 1. The operating conditions (i.e. temperature and initial surfactant concentration) are listed in Table 2.1. After incubating the four solutions in the water bath for 18 hours, the two coexisting micellar phases were withdrawn carefully using syringe and needle sets. Assuming that radiolabeled anti-Tf antibodies remained bound to gold nanoparticles throughout the partitioning experiments, the amount of AuP in each phase was determined by measuring the amount of radioactivity in each phase using the Cobra Series Auto-Gamma Counter.

Table 2.1. Operating conditions, Triton X-114 concentrations in the top and bottom phases, and masses of the top and bottom phases for the partitioning experiments.

Operating Conditions		**Experimental Values Obtained for DNA Partitioning**			
Temperature (˚C)	**Initial Triton X-114 Concentration (% w/w)**	**Triton X-114 Concentration in the Top Phase (% w/w)**	**Triton X-114 Concentration in the Bottom Phase (% w/w)**	**Mass of the Top Phase (g)**	**Mass of the Bottom Phase (g)**
36.1	9.89	0.022 ± 0.001	19.9 ± 0.8	1.65 ± 0.02	1.70 ± 0.02
34.3	8.66	0.020 ± 0.002	16.5 ± 1.1	1.60 ± 0.02	1.72 ± 0.04
32	7.83	0.026 ± 0.001	16.7 ± 0.3	1.58 ± 0.03	1.72 ± 0.06
30	7.20	0.034 ± 0.001	13.4 ± 2.1	1.66 ± 0.01	1.69 ± 0.02
29.1	6.15	0.038 ± 0.001	13.1 ± 1.8	1.51 ± 0.01	1.80 ± 0.01
26.7	5.29	0.076 ± 0.001	10.8 ± 0.4	1.66 ± 0.02	1.73 ± 0.02

2.2.4. Partitioning Transferrin

To determine the partition coefficient of Tf in the ATPMS, the same partitioning experiment was performed, except that 5 ng of radiolabeled Tf was added instead of the colloidal gold nanoparticles bound to radiolabeled anti-Tf antibodies. Furthermore, to enhance the partitioning of Tf in the ATPMS, the above partitioning experiments were also performed in the presence of nonradioactive AuP (colloidal gold nanoparticles bound to unlabeled anti-Tf antibodies). For these experiments, 100 µL of nonradioactive AuP were added to the micellar solutions, and the solutions were mixed prior to the addition of 5 ng of radiolabeled Tf. After phase separation, the concentration of Tf in each phase was determined by measuring the amount of radioactivity in each phase using the Cobra Series Auto-Gamma Counter.

2.2.5. Concentrating Gold Probes and Transferrin

By altering the volume ratio of the partitioning experiments, colloidal gold nanoparticles bound to radiolabeled anti-Tf antibodies and radiolabeled Tf were concentrated in the top, micelle-poor phase. The same protocols described in *2.2.3. Partitioning Colloidal Gold Probes* and *2.2.4. Partitioning Transferrin* were used, except that the initial Triton X-114 surfactant concentrations and operating temperatures were varied in order to achieve a 1/9 volume ratio. For the concentration experiments, solutions of 9.50% w/w Triton X-114 in PBS were used and incubated at 26.1°C for 18 hours.

2.2.6. Preparing Lateral-Flow Immunoassay Test Strips

There are two different approaches for the LFA: the sandwich assay and the competition assay. In this study, we implemented the competition assay. In the competition LFA assay, as

shown schematically in Figure 1.3, the entire target of interest, or a portion of the target (such as a nontoxic chain of a toxin molecule), is immobilized on a nitrocellulose membrane in the form of a line, called the test line. Secondary antibodies specific to the primary antibody on the colloidal gold nanoparticles are also immobilized on the nitrocellulose membrane in the form of a line, called the control line. In LFA, a sample first comes into contact with the AuP. If the target molecules are present in the sample, they would first bind to their specific antibodies immobilized on the colloidal gold nanoparticles. If the sample has enough target molecules to saturate the target-specific antibodies immobilized on the colloidal gold nanoparticles, the target-specific antibodies in the AuP cannot bind to the immobilized target molecules, and hence do not form a visual band at the test line. This indicates a positive result (Figure 1.3a). Alternatively, if the sample does not contain the target molecules at a concentration that saturates the target-specific antibodies immobilized on the colloidal gold nanoparticles, the target-specific antibodies in the AuP can bind to the immobilized target, and form a visual band at the test line indicating a negative result (Figure 1.3b). Furthermore, regardless of the presence of the target molecule in the sample, AuP will bind to the immobilized secondary antibodies on the control line, which indicates a valid test. The LFA test strips used in this study were prepared using a similar approach to that of Schuurs and coworkers [75].

2.2.7. Transferrin Lateral-Flow Immunoassay

The operating condition that yielded a 1/9 volume ratio and was used for performing the concentration step prior to the detection step resulted in Tf and AuP being concentrated in the top, micelle-poor phase that had a Triton X-114 concentration of 0.065% w/w in PBS. Since surfactant can aid lateral flow and since we wanted to be consistent between the LFA performed

with or without the concentration step, Tf solutions in 0.065% w/w Triton X-114 in PBS were used to perform the immunoassay without the pre-concentration step. For the LFA, solutions of Tf diluted in 0.065% w/w Triton X-114 in PBS were first prepared. 45 µL of the Tf solutions were then added to 5 µL of the AuP solution and 10 µL of test buffer (0.2% BSA, 0.3% Tween20, 0.2% sodium azide, 0.1% polyethylene glycol, 0.1 M Trizma base, pH 8), which was used to facilitate the flow of the samples through the test strips. The resulting solutions were mixed and incubated for 18 hours. This incubation time was chosen to allow the same time for anti-Tf antibodies present on the AuP to bind to Tf with or without the concentration step. After the incubation period, an LFA test strip was dipped vertically into each solution so that only the sample pad would come in contact with the solution. After 15 minutes, the test strips were taken out of the solution, and an image of each strip was immediately taken by a Canon EOS 1000D camera (Canon U.S.A., Inc., Lake Success, NY).

2.2.8. Combining Concentration of Transferrin with the Lateral-Flow Immunoassay

To combine the concentration step with the detection step, Tf was first concentrated following a similar protocol as mentioned previously by first adding 50 µL of AuP to the aqueous micellar solutions, followed by mixing the solutions well. Next, various amounts of Tf were added to each solution to obtain appropriate initial concentrations of Tf. For these experiments, 5 mL solutions of 9.50% w/w Triton X-114 in PBS were used and incubated at 26.1°C for 18 hours. At these operating conditions, a volume ratio of 1/9 (0.111) was obtained. After phase separation, the top phases were withdrawn carefully using syringe and needle sets. The LFA was performed as described in *2.2.7. Transferrin Lateral-Flow Immunoassay* except instead of using 45 µL of the Tf solutions diluted in 0.065% w/w Triton X-114 in PBS and 5 µL

of AuP, 50 µL of the withdrawn top, micelle-poor phases were added to 10 µL of test buffer before a test strip was immediately dipped vertically into each solution. Since the amount of AuP used affects the detection limit of LFA, 50 µL of the top, micelle-poor phase was used, since it contained approximately the same amount of AuP utilized in the LFA without the concentration step.

2.3. Results and Discussion

2.3.1. Partitioning Gold Probes in an Aqueous Two-Phase Micellar System

To quantify the partitioning behavior of a molecule in an ATPMS, the partition coefficient, K_m, is evaluated, which is defined as follows:

$$K_m \equiv \frac{C_{m,t}}{C_{m,b}} \tag{2.1}$$

where $C_{m,t}$ and $C_{m,b}$ are the concentrations of the molecule in the top and bottom phases, respectively. Previously, the partitioning behavior of a spherical, water-soluble molecule in a nonionic ATPMS was studied, and it was shown that the partition coefficient could reasonably be predicted using the following expression [54]:

$$K_s^{EV} = \exp\left[-\left(\Phi_t - \Phi_b\right)\left(1+\frac{R_s}{R_0}\right)^2\right] \tag{2.2}$$

where Φ_t and Φ_b are the surfactant volume fractions in the top and bottom phases, respectively, R_s is the hydrodynamic radius of a spherical molecule, and R_0 is the cross-sectional radius of each cylindrical micelle. The above expression was derived considering only the repulsive, steric, excluded-volume interactions that operate between the spherical molecules, such as

spherical proteins, and the cylindrical micelles. As noted previously, water-soluble proteins have been shown to partition fairly evenly between the two phases of an ATPS [40, 43-44, 54, 60], which in turn would result in limited concentration of such proteins into one of the two phases. However, the hydrodynamic radius of AuP utilized in this study (28 nm) is large. Accordingly, based on this radius, the cross-sectional radius of Triton X-114 micelles (23.4 Å, [58]), and the one-to-one correspondence between operating temperature and $(\Phi_t-\Phi_b)$ found previously [58], extremely large (>> 1000) partition coefficients of AuP as a function of temperature were predicted using Equation 2.2. Therefore, similar to the partitioning of DNA fragments and viruses in ATPMS [58, 72, 76], the entrainment of micelle-poor domains in the macroscopic micelle-rich phase were expected to have a significant impact on the partitioning behavior of AuP.

Due to the small density difference and interfacial tension between the micelle-rich and micelle-poor domains, even after waiting a long time, macroscopic phase separation equilibrium is not attained. As a result, some micelle-poor domains are entrained in the macroscopic micelle-rich phase, and similarly, some micelle-rich domains are entrained in the macroscopic micelle-poor phase. If AuP partition extremely into the micelle-poor domains, as predicted by Equation 2.2, the concentration of AuP in the micelle-poor domains would be orders-of-magnitude greater than that in the micelle-rich domains. Therefore, the effect of entrained micelle-poor, AuP-rich domains on the measured concentration of AuP in the macroscopic, micelle-rich, AuP-poor phase would be very significant, while the effect of entrained micelle-rich, AuP-poor domains on the measured concentration of AuP in the macroscopic, micelle-poor, AuP-rich phase would be negligible. Defining x as the volume fraction of *micelle-poor domains*

entrained in the bottom, macroscopic micelle-rich phase, the newly predicted partition coefficient could be written as follows [58, 76]:

$$K_{AuP}^{EV+Ent} = \frac{K_{AuP}^{EV}}{1 + x \cdot \left(K_{AuP}^{EV} - 1 \right)} \tag{2.3}$$

where K_{AuP}^{EV} is the partition coefficient of AuP based only on excluded-volume interactions, and it is equal to the ratio of $C_{AuP,mp}^{EV}$ to $C_{AuP,mr}^{EV}$. For large values of K_{AuP}^{EV}, as in the case of AuP in ATPMS, Equation 2.3 simplifies to:

$$\lim_{K_{AuP}^{EV} \to \infty} K_{AuP}^{EV+Ent} \approx \frac{1}{x} \tag{2.4}$$

Equation 2.4 indicates that the partition coefficient of AuP is only dependent on *x* if (i) entrainment is present and (ii) K_{AuP}^{EV} is much, much greater than 1. Blankschtein and coworkers demonstrated that *x* is only a function of the volume ratio [76]. Therefore, if the volume ratio is maintained at 1 for all temperatures, the measured partition coefficients for AuP should not change by varying the operating temperature. Figure 2.2 shows the partition coefficients of AuP obtained experimentally at various operating temperatures, while the volume ratio was maintained at approximately 1. As indicated in Figure 2.2, the partitioning behavior of AuP in the Triton X-114 ATPMS is approximately independent of the operating temperature, suggesting that the partitioning of AuP is driven by the steric, excluded-volume interactions that operate between AuP and micelles, but is limited by entrainment.

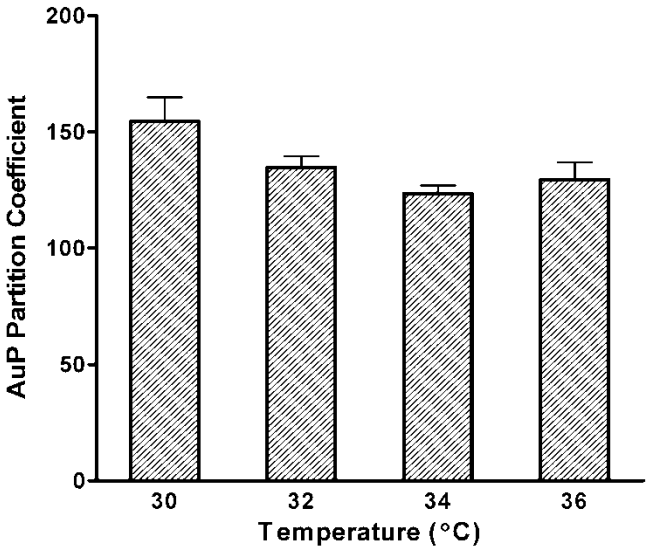

Figure 2.2. Experimentally measured partition coefficients for gold probes at varying temperatures. Error bars represent standard deviations from triplicate measurements.

2.3.2. Partitioning Transferrin in an Aqueous Two-Phase Micellar System

As mentioned previously, unlike large hydrophilic macromolecules, such as genomic DNA fragments and viruses, water-soluble proteins have been shown to partition fairly evenly between the two phases of an ATPS. Therefore, in this study, as shown schematically in Figure 2.1, we investigated utilizing AuP, or colloidal gold nanoparticles bound to Tf-specific antibodies, to enhance the partitioning of Tf in the Triton X-114 ATPMS. In this approach, if all the Tf molecules are successfully captured by the AuP, the same partition coefficients as those obtained for AuP (Figure 2.2) are expected for Tf. Figure 2.3 shows the partition coefficients of Tf obtained experimentally, with or without utilizing AuP, at the operating temperatures used previously for the AuP partitioning experiments. Although the measured partition coefficients of Tf increased when AuP were used, they were significantly lower than those obtained for AuP alone, which indicates that not all Tf molecules were captured by anti-Tf antibodies bound to gold nanoparticles. This could be due to two reasons. The first reason is that not enough anti-Tf

antibodies bound to gold nanoparticles were present in the solution to capture all the Tf molecules. Based on our characterization of AuP using radiolabeled anti-Tf antibodies, approximately a 134-fold molar excess of anti-Tf antibody was used. However, the orientations of the antibodies on the surfaces of gold nanoparticles are unknown, since the three main amino acids thought to be responsible for protein-gold conjugation, namely, lysine, tryptophan, and cysteine [77], are at various locations on the anti-Tf antibodies. Therefore, some of the anti-Tf antibodies might not be able to bind to Tf due to the steric hindrance from the gold nanoparticles. To improve the efficiency of capturing Tf, and thus enhance Tf partitioning further, other conjugation methods must be investigated where more control over the orientation of the antibodies may be applied. The second reason could be a low affinity between the anti-Tf antibodies used in these studies and Tf. Therefore, to further improve Tf partitioning, anti-Tf antibodies with higher affinity for Tf could be utilized. Nonetheless, since the measured values of the partition coefficients of AuP are much greater than 1, they can still be exploited in a novel fashion to improve the Tf LFA detection limit as described in the following sections.

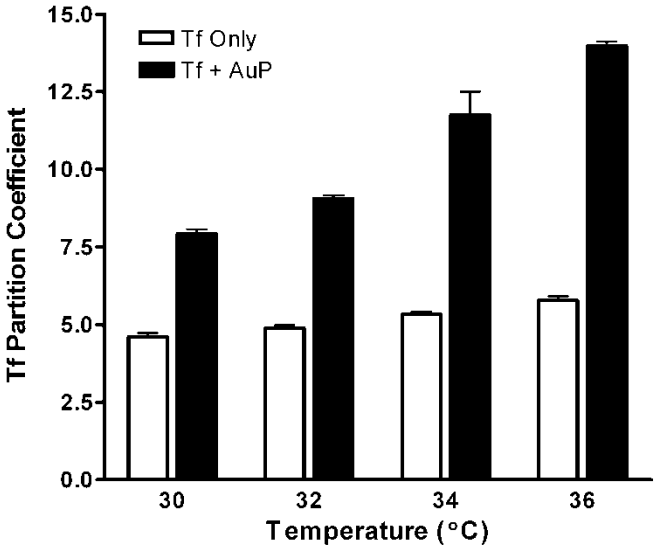

Figure 2.3. Experimentally measured partition coefficients of Tf at varying temperatures without (white bars) and with (black bars) utilizing gold probes. Error bars represent standard deviations from triplicate measurements.

2.3.3. Concentrating Gold Probes and Transferrin by Manipulating the Volume Ratio

By utilizing the mass balance of species *i* in the ATPS, in an approach similar to that developed by other researchers [34], an expression for the concentration factor, that is, the concentration of molecule *i* in the top phase ($C_{i,t}$), divided by the initial concentration of molecule *i* ($C_{i,0}$), was derived:

$$Concentration\ factor \equiv \frac{C_{i,t}}{C_{i,0}} = \frac{\frac{V_t}{V_b}+1}{\frac{V_t}{V_b}+\frac{1}{K_i^m}} \tag{2.5}$$

where V_t and V_b are the volumes of the top and bottom phases, respectively, and K_i^m is the measured partition coefficient of species *i* obtained experimentally. For large values of K_i^m, the concentration factor for molecule *i* could be approximated as follows:

$$Concentration\ factor \equiv \frac{C_{i,t}}{C_{i,0}} \approx 1 + \frac{1}{\frac{V_t}{V_b}} \tag{2.6}$$

Therefore, based on Equation (2.6), and the large values of the partition coefficients of the AuP, K^m_{AuP}, obtained experimentally (Figure 2.2), the concentration factor for gold probes can be manipulated by solely varying the volume ratio. However, Equation (2.6) cannot be applied to Tf, with or without utilizing AuP, since much smaller Tf partition coefficients were obtained (Figure 2.3). Figure 2.4 shows the concentration factors obtained experimentally with an approximately 1/9 volume ratio for AuP, and Tf molecules, with or without utilizing AuP. As indicated in Figure 2.4, there is reasonable agreement between the experimentally measured concentration factor of AuP and the prediction based on Equation (2.6). This agreement is not observed for Tf, with or without utilizing AuP, due to the lower partition coefficients, which prevented the Tf molecules from being significantly concentrated. However, note that increasing the efficiency of capturing Tf molecules is expected to increase the Tf partition coefficients when AuP are utilized. This, in turn, would allow the Tf molecules to be concentrated to the same extent as the AuP. However, as described in the next sections, successfully concentrating the AuP themselves can still be exploited to improve the detection limit of LFA.

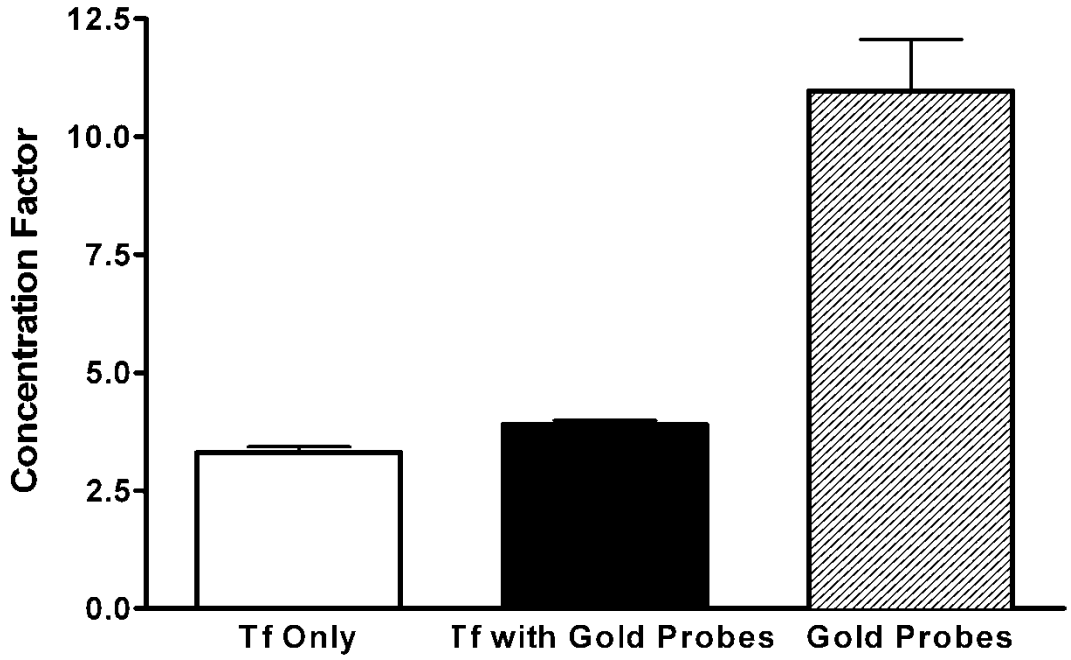

Figure 2.4. Concentration factors for the gold probes (crossed bars) and Tf, without (white bars) and with (black bars) the use of gold probes with a 1/10 volume ratio. Error bars represent standard deviations from triplicate measurements.

2.3.4. Detecting Transferrin via the Lateral-Flow Immunoassay

In this study, we implemented the competition assay to detect Tf in-solution. To establish the limit of Tf detection via LFA, test strips were prepared by utilizing rabbit polyclonal anti-goat IgG antibody and Tf. The results of LFA performed are shown in Figure 2.5. As mentioned previously, the top line, which contains immobilized rabbit polyclonal anti-goat IgG antibody, is the control line, indicating a valid test. In the competition LFA, as shown schematically in Figure 1.3, Tf was immobilized on the nitrocellulose membrane on the test line. If the solution being tested contained enough Tf molecules to saturate the anti-Tf antibodies bound to the colloidal gold nanoparticles, then these anti-Tf antibodies could not bind to the immobilized Tf molecules at the test line, and hence, would not form a visual band at the test

line. This indicated a positive result, which was observed for solutions with Tf concentrations as low as 0.5 µg/mL (Figure 2.5e). Alternatively, if the sample did *not* contain Tf at a concentration that saturated the anti-Tf antibodies bound to the colloidal gold nanoparticles, then some of these anti-Tf antibodies would bind to the immobilized Tf at the test line, and therefore, form a visual band indicating a negative result. This was observed for the negative control, which did not contain any Tf (Figure 2.5a), as well as for solutions with Tf concentrations of 0.1 and 0.05 µg/mL (Figure 2.5f and g). This indicated a detection limit of approximately 0.5 µg/mL for the Tf LFA performed without a prior concentration step.

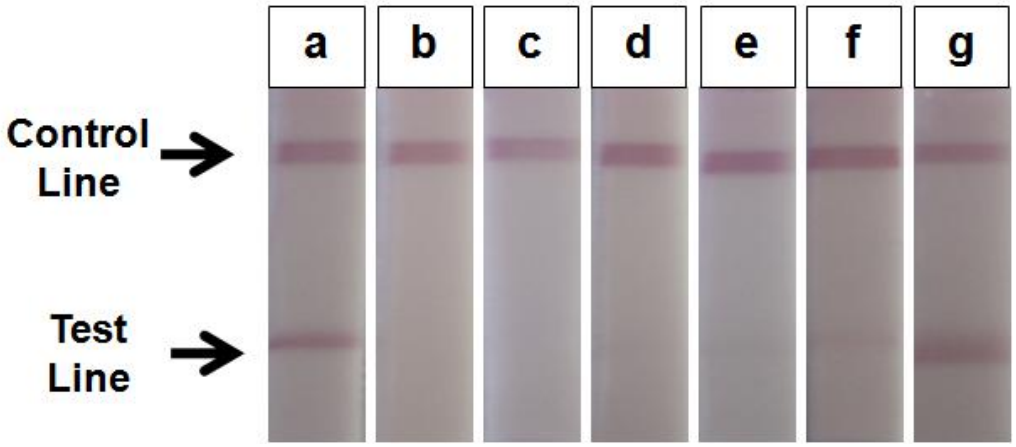

Figure 2.5. LFA used to detect Tf without a prior concentration step. The negative control without any Tf is shown in panel (a). The remaining solutions contained Tf at concentrations of (b) 10, (c) 5, (d) 1, (e) 0.5, (f) 0.1, and (g) 0.05 µg/mL.

2.3.5. Concentrating Gold Probes and Transferrin Prior to the Lateral-Flow Immunoassay

After establishing the detection limit of the Tf LFA, we investigated the possibility of improving the detection limit of LFA if an ATPMS was utilized to concentrate AuP and Tf molecules prior to the detection step. As shown previously, while AuP were successfully concentrated in the ATPMS in a predictive manner, lower concentration factors were obtained

for Tf with or without utilizing AuP. However, as explained below, the successful concentration of AuP was still exploited to improve the LFA detection limit of Tf.

In the competition LFA, the deciding factor for detecting Tf in-solution is saturation of the anti-Tf antibodies bound to colloidal gold nanoparticles with Tf molecules. If these anti-Tf antibodies bound to colloidal gold nanoparticles are not saturated with Tf, then they would bind to the immobilized Tf at the test line, and form a visual band indicating a negative result. As shown in Figure 2.5g, in the case of the solution with a Tf concentration of 0.05 µg/mL, the anti-Tf antibodies were not saturated with Tf molecules, and therefore, the test line appeared for this Tf concentration, indicating a false negative result. Therefore, to detect Tf at the concentration of 0.05 µg/mL, the anti-Tf antibodies bound to colloidal gold nanoparticles must be saturated with Tf molecules. One approach is to add more Tf molecules by utilizing a larger volume of the 0.05 µg/mL Tf solution for performing the LFA, while holding the AuP volume constant.

In the previously mentioned studies, LFA was performed by adding 45 µL of Tf solutions to 5 µL of the AuP and 10 µL of test buffer before dipping an LFA test strip into the mixture. Note that Tf was successfully detected at a concentration of 0.5 µg/mL (Figure 2.5e) by utilizing 45 µL of the 0.5 µg/mL Tf solution, indicating that the anti-Tf antibodies bound to colloidal gold nanoparticles were successfully saturated with Tf. Therefore, in the case of a 0.05 µg/mL Tf solution, which is 10 times more dilute, to ensure that there are enough Tf molecules to saturate the anti-Tf antibodies bound to colloidal gold nanoparticles, instead of 45 µL of the 0.05 µg/mL Tf solution, 45 µL x 10 = 450 µL of the 0.05 µg/mL Tf solution could be added to 5 µL of the AuP and 10 µL of test buffer. The solution would also need to be thoroughly mixed to ensure that the antibodies can interact with the Tf molecules in the dilute solution. However, only a limited volume (approximately 50 µL) can be used in the LFA test strip before the strip becomes

saturated with liquid, leading to the flow stopping. Therefore, although the anti-Tf antibodies bound to colloidal gold nanoparticles would become saturated with Tf by using a 10 times larger volume of the 0.05 µg/mL Tf solution, only a small portion of the AuP would pass through the strip when 50 µL of the solution is used, since the AuP would be diluted 10-fold in the 450 □L solution. As a result, the control line will not appear, indicating an invalid test. To overcome this problem, the ATPMS was used to concentrate the AuP into the top, micelle-poor phase prior to the LFA. As shown in Figure 2.4, by using an approximately 1/9 volume ratio, the AuP were concentrated in the top, micelle-poor phase by approximately 10-fold. This would counteract the effect of the 10-fold dilution of the AuP and allow detection at the control line. It should be noted that in this setup, it is not as important to capture all the Tf molecules, but rather to recover almost all of the AuP at a high enough concentration that a valid result can be obtained when only 50 µL of the solution is used.

To combine the concentration step with LFA, 9.50% w/w Triton X-114 in PBS solutions that contained AuP and had different initial concentrations of Tf were prepared. The solutions were mixed well, and subsequently incubated at 26.1°C for 18 hours. After phase separation, which yielded a 1/9 volume ratio, the top, micelle-poor, AuP-rich phases were withdrawn using syringe and needle sets, and were consequently used in the LFA as described previously. The results of the LFA with the prior concentration step are shown in Figure 2.6. While the test line appeared for the negative control solution, which did not contain any Tf, indicating a negative result, the test line did *not* appear for the decreasing concentration of Tf until the concentrations of 0.01 and 0.005 µg/mL (Figure 2.6h and i). This indicated a detection limit of approximately 0.05 µg/mL for the Tf LFA when combined with the ATPMS, which represented a 10-fold improvement of the detection limit of the LFA assay. It should be noted that, in this proof-of-

concept study, a volume ratio of only 1/9 was utilized to demonstrate the improvement of the concentration step on LFA's detection limit. In the future, even lower volume ratios may be used to yield greater concentration factors of the AuP that can then lead to even lower detection limits. Furthermore, while phase separation of an ATPS could be sped up via low-speed centrifugation [78], the ultimate goal of this approach is to enhance the detection of protein markers at the PON without using any laboratory equipment. Accordingly, other ATPS could instead be utilized and optimized to achieve rapid separation within the time frame of typical LFA diagnostic tests without the need for centrifugation.

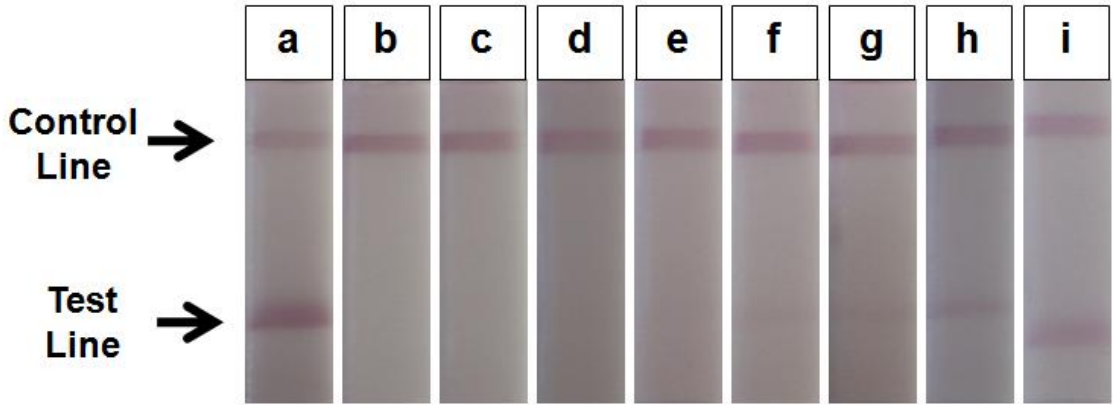

Figure 2.6. LFA used to detect Tf with the prior concentration step. The negative control without any Tf is shown in panel (a). The remaining solutions contained Tf at concentrations of (b) 10, (c) 5, (d) 1, (e) 0.5, (f) 0.1, (g) 0.05, (h) 0.01, and (i) 0.005 µg/mL.

2.4 Conclusions

Concentrating proteins, such as food allergens and protein toxins, prior to a detection step via LFA may improve the detection limit of the immunoassay. In this study, the partitioning and concentration of a model protein, namely Tf, using a novel modification in the Triton X-114 ATPMS was investigated. Specifically, anti-Tf antibodies bound to colloidal gold nanoparticles, or AuP, were utilized to enhance the partitioning of Tf in the ATPMS. First, to understand the partitioning behavior of AuP in the ATPMS, we compared experimentally measured partition

coefficients of AuP with the theoretical predictions obtained from a model developed previously for partitioning of spherical molecules in micellar systems. The agreement between theory and experiment indicated that the partitioning behavior of AuP in the nonionic micellar system is primarily driven by repulsive, steric, excluded-volume interactions that operate between the micelles and AuP, but is limited by the entrainment of micelle-poor, AuP-rich domains in the macroscopic, micelle-rich phase. Subsequently, we investigated the partitioning of Tf in the ATPMS with or without utilizing the AuP. Although Tf partitioning was enhanced by approximately 2-fold when AuP were utilized, it was shown that only 39% to 49% of Tf molecules was captured by the AuP, which resulted in limited improvement of Tf partitioning in the micellar system. Therefore, to enhance Tf partitioning further by increasing the percentage of Tf molecules captured, AuP with higher affinity to Tf must be utilized and the orientation of the conjugated molecules must be examined. However, even with the current system, we discovered a novel approach to improve the detection limit of Tf. Specifically, by decreasing the volume ratio from 1 to approximately 1/9, AuP were concentrated in the top, micelle-poor phase by approximately 10-fold in a predictive manner, and although Tf molecules were not concentrated in the top phase as extremely, the successful concentration of AuP into the top, micelle-poor phase improved the detection limit of LFA by approximately 10-fold by being able to concentrate the AuP that were saturated with Tf. In the future, the operating conditions could be manipulated to obtain even lower volume ratios, which in turn should result in obtaining higher concentration factors of AuP that yield even lower detection limits of LFA. Furthermore, ATPS that yield rapid phase separation could be utilized, so that the complete detection assay, including the concentration step, could be completed within 30 minutes. We believe once optimized, the novel approach of utilizing ATPS to concentrate target proteins prior to the

detection step could significantly improve the sensitivity of LFA, which in turn, could enhance its effectiveness as a PON assay in detecting target proteins in various sample matrices.

Chapter 3: Concentrating Bacteriophage M13 Using an Aqueous Two-Phase Polymer-Salt System to Improve Detection with the Lateral-Flow Immunoassay

3.1. Introduction

Viruses are infectious agents responsible for many various medical ailments and diseases, such as AIDS, the common cold, herpes, and influenza. A means to rapidly and accurately detect infectious agents and pandemic pathogens at the point-of-care (POC) could result in better patient management, such as timely use of appropriate antiviral treatments and isolation of confirmed cases, to aid in preventing outbreaks [13-14]. Viruses, such as the Ebola and Marburg viruses, may also be used as dangerous weapons in biological warfare. Thus, frontline military personnel require a means to rapidly detect these agents when advancing in hostile territories in the form of a portable viral detection device.

One detection method that has gained much attention in recent years due to its ease of use, rapid time to result, and minimal power and laboratory equipment requirements is the lateral-flow immunoassay (LFA). However, studies have shown that the sensitivity of LFA in detecting viruses is inferior to the gold standards of viral culture and real-time PCR [14, 18, 23-27]. Therefore, in order to use LFA as a point-of-care solution for viral detection, the sensitivity of LFA must first be improved. A practical solution for increasing the sensitivity of LFA is to concentrate the target virus in a solution prior to the detection step.

Aqueous two-phase systems (ATPS) can be utilized to concentrate biomolecules. Previously, in a proof-of-principle study, we investigated the use of an aqueous two-phase micellar system using Triton X-114 surfactant to concentrate a model virus, namely bacteriophage M13 (M13), prior to its detection via LFA [79]. Although partitioning of viruses

in aqueous two-phase systems has been previously studied, our work previously reported was the first time the established technologies of LFA and aqueous two-phase systems have been combined. In fact, aqueous two-phase systems have generally been examined for large-scale biotechnological applications [34, 38-39, 43-44, 58, 71] and not small-scale diagnostic applications. Nonetheless, aqueous two-phase systems are appropriate for a POC device, as they involve liquid-liquid extractions making them scalable (to require minimal sample volume), and could be designed to require minimal training and power.

Despite our previous success in improving the viral sensitivity of the LFA by employing an aqueous two-phase micellar system with Triton X-114 surfactant [79], there was an aspect of the concentration method that still needed to be improved from our proof-of-principle study before it could be practically implemented. Specifically, the aqueous two-phase micellar system had phase separation times on the order of hours, which is a result of the low density difference and low interfacial tension between the two phases. Since the micelle-poor rich and micelle-poor domains move up or down accordingly to density difference, the low density difference makes it more difficult for the macroscopic separation of the two-phases. Furthermore, the low interfacial tension allows for greater surface area between the two phases. This consequently allows for more entrained domains of the micelle-rich phase within the micelle-poor phase and vice versa, making it more difficult to form two-distinct macroscopic phases due to increased entrainment.

In this study, we employ the use of another ATPS, one composed of polymer and salt, which phase separates on the order of minutes and is more practical to be implemented for improving point-of-care detection. The aqueous two-phase polymer-salt system was formed using polyethylene glycol (PEG) polymer and potassium phosphate salt. However, the PEG-salt system has one disadvantage which previously prevented its use in being combined with the

LFA. Due to the high-salt content of the solution, the colloidal gold nanoparticles used as the colorimetric indicator in the LFA lose their stability and aggregate in-solution. In this study, we developed modified colloidal gold nanoparticles designed to have increased stability in high-salt solutions. We subsequently investigated the PEG-salt system for concentrating bacteriophage M13 as a model virus to improve the LFA detection of M13.

Macromolecules partition in PEG-salt systems based on hydrophobicity [61] and size [66]. For example, hydrophilic proteins partition more into the bottom polymer-poor, salt-rich phase of PEG-salt systems [61]. Since M13 contains an outer hydrophilic coat [67], M13 is expected to partition into the bottom, polymer-poor, salt-rich phase. Furthermore, large linear polymers form a net in solution and limits large macromolecules from being contained within the polymer-rich phase [66]. Thus, large viral particles are expected to be driven to the bottom, polymer-poor phase due to the excluded-volume interactions that operate between the viral particles and the polymer molecules in the top polymer-rich phase. M13 can thus be concentrated in the bottom, polymer-poor phase by manipulating the volume ratio, defined as the volume of the bottom, polymer-poor phase divided by that of the top, polymer-rich phase.

After ensuring that we could concentrate M13 in the aqueous two-phase polymer-salt system, we developed an LFA for the detection of M13 in-solution. However, before the PEG-salt system could be combined with LFA, the colloidal gold probes (AuP) that were used as the colorimetric indicator needed to be further stabilized. In solutions of low salt concentration, the AuP remain stable due to electrostatic repulsions that result from their negatively charged surfaces which are attributable to citrate ions that remain adsorbed on the nanoparticles in the synthesis process [80]. However, due to the high salt concentration of the aqueous two-phase polymer-salt system, the salt ions screen the electrostatic repulsions between two charged

colloidal gold nanoparticles. Due to these reduced electrostatic repulsions, the AuP are allowed to more closely approach each other, which consequently increases their van der Waal attractions and results in aggregation of the AuP. To overcome this, one approach is to increase the repulsions between AuP by coating the AuP with a layer of PEG on the surface. The PEG layer provides steric repulsions between AuP to effectively prevent them from aggregation. In this study, the AuP were coated with PEG prior to coating with antibodies specific for the target virus.

Once the AuP were PEGylated, we investigated the LFA detection limit of M13 using these modified gold probes. Subsequently, M13 was concentrated using the aqueous two-phase polymer-salt system prior to the detection step to investigate the effect of the concentration step on the LFA's detection limit. To the best of our knowledge, the results reported in this study represent the first time LFA has been combined with an aqueous two-phase system composed of polymer and salt constituents and the first time that PEGylated AuPs have been employed for use in the LFA.

3.2. Materials and Methods

3.2.1. Bacteria and Bacteriophage M13 Culture

Escherichia coli bacteria (American Type Culture Collection, ATCC, Manassas, VA) were incubated in 6 mL of lysogeny broth (LB, 10 g/L tryptone (BD, Franklin Lakes, NJ), 5 g/L yeast extract (BD), and 10 g/L NaCl) media at 37°C and 240 RPM in a shaker incubator for 12 hours. This bacteria solution was then used in the plaque assay to quantify the concentration of M13 (see *3.2.2. Bacteriophage M13 Quantification*). Additionally, in order to culture M13 (ATCC), 10 µL of the stock M13 solution was added to *Escherichia coli* bacteria solution grown

in LB media for 12 hours as described above. The mixture was then incubated in a shaker incubator at 37°C and 240 RPM for 5 hours. The solution was then centrifuged at 4°C and 8000g for 15 min to remove the bacteria. The supernatant containing M13 was collected and filtered using a 0.22 µm syringe filter (Millipore, Billerica, MA). All reagents and materials were purchased from Sigma-Aldrich (St. Louis, MO) unless otherwise noted.

3.2.2. Bacteriophage M13 Quantification

The plaque assay was used to quantify the concentration of M13 in a solution [81]. In this assay, 100 µL of a diluted sample with an unknown concentration of M13 was added to 200 µL of a bacteria solution and 3 mL of soft LB agar (LB, with 0.3% w/v agarose (Promega, Madison, WI)). This solution was then mixed and poured onto a Petri dish covered with hard LB agar (LB, with 1.2% w/v agarose (Promega)). This assay relies on the fact that M13 infects cells, replicates inside them, slows down their growth, and spreads to neighboring cells. Consequently, if a single M13 viral particle is placed in an environment of growing bacteria cells, eventually a plaque or hole will be visible in the opaque yellowish bacteria lawn due to the inhibited growth of bacterial cells that are infected by the replicating bacteriophage. Although many bacteriophages are responsible for one plaque, they all originated from a single infectious viral particle that was initially placed on the hard LB agar. Therefore, the concentration of M13 is reported in plaque forming units (pfu) per mL.

3.2.3. Concentrating Bacteriophage M13 in Aqueous Two-Phase Polymer-Salt Systems

By altering the volume ratio of the aqueous-two phase polymer-salt system, M13 can be concentrated in the bottom, polymer-poor phase. For each concentration experiment, four

identical aqueous solutions composed of 25% w/w PEG8000 (Promega, Madison, WI) and 3.2% w/w potassium phosphate salt (1 to 5 mass ratio of KH_2PO_4 to K_2HPO_4) dissolved in Dulbecco's phosphate-buffered saline (PBS, Invitrogen, pH 7.4, containing 1.47 mM KH_2PO_4, 8.10 mM Na_2HPO_4, 138 mM NaCl, 2.67 mM KCl, and 0.495 mM $MgCl_2$) were prepared. M13 was added to three of the solutions such that the final concentration of the solution was 10^8 bacteriophage particles/mL. The fourth solution served as the control which did not contain any bacteriophage. The four solutions were incubated in a water bath at 37.0 °C, which yields a volume ratio, defined as the volume of the bottom, polymer-poor phase divided by the top, polymer-rich phase, of approximately 10. After thirty minutes, the two coexisting polymer-rich and polymer-poor phases were extracted from the solutions using syringe and needle sets. The concentration of M13 in each phase was determined as described above in *3.2.2. Bacteriophage M13 Quantification*. The concentration experiment which involved the triplicate solutions and control, was repeated three times.

3.2.4. Preparing Colloidal Gold Probes

The colloidal gold nanoparticles were prepared according to Frens [73]. Briefly, 1 mL of a 10% gold (III) chloride hydrate was added to 1 L of 100°C deionized water. 1.5 mL of 12% sodium citrate was then added to reduce the gold chloride into gold atoms, which would subsequently nucleate to form gold colloids. Using this method, a 1 L solution of colloidal gold nanoparticles was obtained, which appeared as a clear, dark cherry-colored solution.

The concentration of the colloidal gold nanoparticle solution was determined by using Beer's Law for a path length of 1 cm:

$$C = \frac{A}{\varepsilon} \qquad (3.1)$$

In Equation (3.1) above, C is the concentration of colloidal gold nanoparticles in mol/liter, ε is the molar extinction coefficient in $M^{-1}cm^{-1}$, and A is the peak absorbance value of the colloidal gold nanoparticles in water. In our studies, the peak absorbance value of the colloidal gold nanoparticles was measured using a spectrophotometer. The molar extinction coefficients are specific to colloidal gold nanoparticle size and were taken from a data sheet provided by BBInternational Life Sciences (Madison, WI), a manufacturer of colloidal gold nanoparticles. Some of the molar extinction coefficients from this data sheet are shown in Table 3.1. The values in the data sheet were extrapolated from mean-free-path corrected Mie-theory calculations performed by Wolfgang Haiss at the University of Liverpool [82]. The average diameter of the colloidal gold nanoparticles was measured using dynamic light scattering measurements (DLS) with a Zetasizer Nano ZS particle analyzer (Malvern Instruments Inc, Westborough, Massachusetts) following the manufacturer's instructions.

Table 3.1. Colloidal gold nanoparticle extinction coefficients.

diameter (nm)	ε (M^{-1} cm^{-1})	diameter (nm)	ε (M^{-1} cm^{-1})
31	4.00E+09	41	1.01E+10
32	4.44E+09	42	1.09E+10
33	4.91E+09	43	1.18E+10
34	5.42E+09	44	1.27E+10
35	5.96E+09	45	1.37E+10
36	6.54E+09	46	1.47E+10
37	7.16E+09	47	1.58E+10
38	7.82E+09	48	1.69E+10
39	8.52E+09	49	1.81E+10
40	9.26E+09	50	1.94E+10

After quantifying the colloidal gold nanoparticles using the method described above, the results were verified with another concentration quantification method by using a mass balance of the nanoparticles. Since the nanoparticles are spheres, the total number of nanoparticles can be

calculated from the measured nanoparticle mass and radius. The mass balance and corresponding equation is shown below.

$$\text{number of particles} \cdot \text{volume per particle} \cdot \text{density} = \text{total mass} \qquad (3.2)$$

$$n\left(\frac{4\pi R^3}{3}\right)\rho = m \qquad (3.3)$$

The radius of the nanoparticles, *R*, was determined using DLS measurements. The density of the nanoparticles, ρ, was taken to be approximately the same as the density of gold, which is equal to 19.3 g/cm^3. The mass of the colloidal gold nanoparticles, *m*, was determined through freeze-drying a known volume of colloidal gold nanoparticle solution using a lyophilizer. The calculated colloidal gold nanoparticle concentration using this method was similar to the results attained from using Beer's Law and the provided molar extinction coefficients listed in Table 3.1.

After the colloidal gold nanoparticles were synthesized and their concentration determined, a polyethylene glycol (PEG) layer was added to the particle surfaces for increased particle stability in high-salt containing solutions. Briefly, the pH of a 1 mL colloidal gold nanoparticle solution was adjusted to pH 7.2 using 10x PB buffer (6.7 mM KH_2PO_4, 13.7 mM K_2HPO_4). In the PEGylation process, both monofunctional and bifunctional PEG polymers were utilized to coat the colloidal gold nanoparticles. Amino-PEG MW 5000 (Nanocs, New York, NY) served as the monofunctional PEG and is able to bind to the colloidal gold nanoparticles through dative bonds via the amine group [80]. In the case of the bifunctional PEG polymer, amino-PEG-maleimide MW 10000 (Nanocs) was used. The amine group binds to the colloidal gold nanoparticles, while the maleimide group binds to free thiols on antibodies. Both monofunctional and bifunctional PEG were added to the colloidal gold nanoparticle solution at a

molar ratio of 5000 PEG polymers per 1 colloidal gold nanoparticle. The solution was then mixed on a shaker for 1 hour.

After PEGylation, antibodies were conjugated to the free ends of the bifunctional PEG on the colloidal gold nanoparticles to complete the synthesis of the colloidal gold probe (AuP). To accomplish this, the PEGylated colloidal gold nanoparticle solution was first adjusted to pH 9 using 0.1 M NaOH. In the case of forming the first gold probe species (AuP_{test}) designed to bind only to the test line, 16 µg of anti-M13 mouse monoclonal antibody (Abcam Inc., Cambridge, MA) at a concentration of 0.2 mg/mL was added to the colloidal gold solution and mixed for 10 min on a shaker. In the case of forming the second gold probe species ($AuP_{control}$) designed to bind only to the control line, 16 µg of goat polyclonal anti-Tf antibody (Bethyl Laboratories, Montgomery, TX) at a concentration of 0.2 mg/mL was added to the colloidal gold solution and mixed for 10 min on a shaker. To prevent nonspecific binding of other proteins to the surfaces of the colloidal gold nanoparticles, 100 µL of 10% w/v bovine serum albumin was added to both the AuP_{test} and $AuP_{control}$ solution and mixed for 15 min on a shaker to block any remaining exposed surfaces on the colloidal gold nanoparticles. The AuP_{test} and $AuP_{control}$ solutions were then centrifuged for 30 min at 4°C and 9000g to remove free antibody and bovine serum albumin. The pellets from both AuP_{test} and $AuP_{control}$ solutions were resuspended in 150 µL of 0.1 M sodium borate buffer at pH 9.0.

3.2.5. Preparing Lateral-Flow Immunoassay Test Strips

Using a similar approach to that of Schuurs and coworkers [75], the LFA test strips were prepared as follows: Rabbit polyclonal anti-goat IgG (Bethyl Laboratories) and mouse monoclonal anti-M13 antibodies (Abcam) were first diluted to 0.4 mg/mL and 0.2 mg/mL,

respectively, by using a 50% w/v sucrose solution. The antibody solutions were then sprayed at their corresponding locations of a nitrocellulose membrane (Sartorius, Goettingen, Germany) using a syringe and PEEK™ tubings (Upchurch Scientific, Oak Harbor, WA). The nitrocellulose membrane was then dried under vacuum for two hours, and left overnight at room temperature and atmospheric pressure to allow the membrane to retain its relaxed form. Subsequently, the treated nitrocellulose membrane, the sample pad (Whatman, Kent, UK) which is where the solution is applied, the absorbance pad (Whatman) which functions as a sink for excessive sample fluid, and adhesive vinyl backing (G&L, San Jose, CA) were assembled, and cut into test strips shown schematically in Figure 1.1 in Chapter 1. Before assembly, the sample pad was incubated overnight in a water solution containing surfactant (0.5% w/v PEG8000 and 0.5% w/v Tween20) and vacuum dried for two hours the following day. This was done to aid in the capillary flow of the sample up the LFA strip.

3.2.6. Bacteriophage M13 Lateral-Flow Immunoassay

To be consistent between the lateral-flow immunoassays performed with or without the concentration step, M13 solutions were prepared in aqueous samples that were extracted from the bottom, polymer-poor phase of a PEG-potassium phosphate salt solution that had phase separated under the same operating conditions as mentioned in *3.2.3. Concentrating Bacteriophage M13 in Aqueous Two-Phase Polymer-Salt Systems*. These M13 solutions were used to perform the LFA without the concentration step. Forty-five µL of these M13 solutions of varying M13 concentration were then added to 10 µL of the AuP_{test} solution, 5 µL of the $AuP_{control}$ solution (see *3.2.4. Preparing Colloidal Gold Probes*) and 25 µL of test buffer (0.2% bovine serum albumin, 0.3% Tween20, 0.2% sodium azide, 0.1% polyethylene glycol, 0.1 M

Trizma base, pH 8), which was used to facilitate the flow of the samples through the test strips. The resulting solutions were mixed, and incubated for 5 minutes before a test strip (see *3.2.5. Preparing Lateral-Flow Immunoassay Test Strips*) was dipped vertically into each solution. After 20 minutes, the test strips were taken out of the solution, and an image of each strip was immediately taken by a Canon EOS 1000D camera (Canon U.S.A., Inc., Lake Success, NY).

3.2.7. Combining Concentration of M13 with the Lateral-Flow Immunoassay

To combine the concentration step with the detection step, M13 was first concentrated following the same protocol as mentioned previously (see *3.2.3. Concentrating Bacteriophage M13 in Aqueous Two-Phase Polymer-Salt Systems*). Various amounts of M13 were added to each solution to obtain appropriate initial concentrations of M13. After phase separation, the bottom, polymer-poor, virus-rich phases were withdrawn carefully using syringe and needle sets. The LFA was performed as described in *3.2.6. Bacteriophage M13 Lateral-Flow Immunoassay*, except instead of using 45 µL of the M13 solutions diluted in a pre-extracted bottom phase, 45 µL of the withdrawn bottom, polymer-poor phases were used.

3.3. Results and Discussion

3.3.1. Concentrating Bacteriophage M13 by Manipulating the Volume Ratio

In an approach similar to that developed by other research groups [34], an expression for the concentration factor, that is, the concentration of virus in the bottom phase divided by the

initial concentration, will now be derived. The starting point in the derivation is the mass balance of M13 in the aqueous two-phase system:

$$C_{M13,0} \cdot (V_t + V_b) = C_{M13,t} \cdot V_t + C_{M13,b} \cdot V_b \qquad (3.4)$$

where V_t and V_b are the volumes of the top and bottom phases, respectively, $C_{M13,0}$ is the initial concentration of M13 in the homogeneous micellar solution prior to phase separation, and $C_{M13,t}$ and $C_{M13,b}$ are the concentrations of M13 in the top and bottom phases, respectively. Dividing both sides of Equation (3.4) by V_t and $C_{M13,b}$ yields the following equation:

$$\frac{C_{M13,0}}{C_{M13,b}} \cdot (1 + \frac{V_b}{V_t}) = \frac{1}{K^m_{M13}} + \frac{V_b}{V_t} \qquad (3.5)$$

where K^m_{M13} is the measured partition coefficient obtained from quantifying the concentration of M13 in each phase and is defined as:

$$K^m_{M13} \equiv \frac{C_{M13,b}}{C_{M13,t}} \qquad (3.6)$$

Rearranging Equation (3.5) to solve for the concentration factor, *CF*, which is defined as the measured concentration of M13 in the bottom phase divided by the initial concentration of M13 prior to phase separation, yields the following equation:

$$CF \equiv \frac{C_{M13,b}}{C_{M13,0}} = \frac{1 + \frac{V_b}{V_t}}{\frac{1}{K^m_{M13}} + \frac{V_b}{V_t}} \qquad (3.7)$$

For large values of K^m_{M13}, the concentration factor could be approximated as follows:

$$CF \equiv \frac{C_{M13,b}}{C_{M13,0}} \approx \frac{1}{\frac{V_b}{V_t}} + 1 \qquad (3.8)$$

Therefore, based on Equation (3.8), if the measured M13 partition coefficients, K_{M13}^{m}, obtained experimentally are large, the concentration factor can be manipulated by varying the volume ratio. In this study, the operating conditions yielded volume ratios of approximately 1/9 in the aqueous two-phase polymer-salt systems. The average measured partition coefficient of M13 was 28 ± 9. The average concentration factor was measured to be 8.8 ± 2.3. Since Equation (3.8) predicts a concentration factor of approximately 10 for a volume ratio of 1/9, there is reasonable agreement between the experimentally measured concentration factor and the predicted value obtained from Equation (3.8).

3.3.3. Detecting Bacteriophage M13 via the Lateral-Flow Immunoassay

After demonstrating that M13 could be concentrated via an aqueous two-phase polymer-salt system, we prepared colloidal gold probes and LFA test strips by utilizing rabbit polyclonal anti-goat IgG for the control line and mouse monoclonal antibody to M13's coat protein pVIII for the test line. The LFA was performed as described in *3.2.6. Bacteriophage M13 Lateral-Flow Immunoassay*, and the results are shown in Figure 3.1. As mentioned previously, the top line, which contains immobilized rabbit polyclonal anti-goat IgG antibody, is the control line, indicating a valid test. The presence of the test line, which contains mouse monoclonal antibody to M13's coat protein pVIII, indicates the presence of M13. As indicated in Figure 3.1, while no test line appeared for the negative control solution (Figure 3.1a), which did not contain any M13, the intensity of the test line decreased with the decreasing concentration of M13 (Figure 3.1b-f) until no test line appeared for the solution containing $1x10^{8}$ pfu/mL (Figure 3.1f). This indicated a detection limit of $5x10^{8}$ pfu/mL for the M13 LFA performed without a prior concentration step.

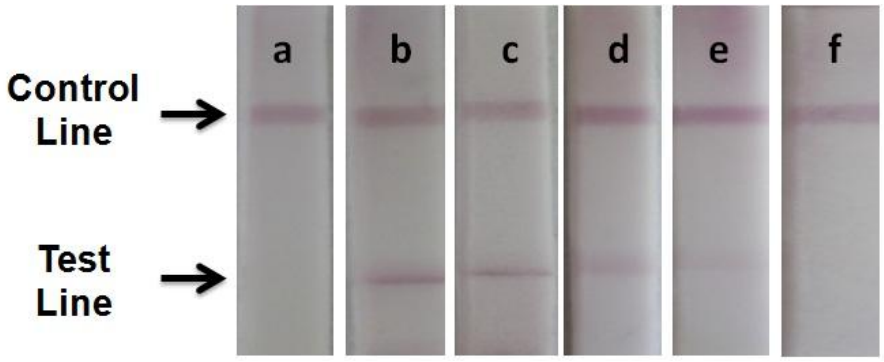

Figure 3.1. LFA used to detect bacteriophage M13 without a prior concentration step. The negative control without any M13 is shown in panel (a). The remaining solutions contained M13 at concentrations of (b) $1x10^{10}$, (c) $5x10^{9}$, (d) $1x10^{9}$, (e) $5x10^{8}$, and (f) $1x10^{8}$ pfu/mL.

3.3.4. Concentrating Bacteriophage M13 Prior to the Lateral-Flow Immunoassay

After establishing the detection limit of the M13 LFA, we investigated improving the sensitivity of the assay by utilizing an aqueous two-phase polymer-salt system to concentrate M13 prior to the detection step. To do so, 25% w/w PEG8000 and 3.2% w/w potassium phosphate salt in PBS solutions with different initial concentrations of M13 were incubated at 37.0°C for 30 minutes. After phase separation, the bottom, polymer-poor, M13-rich phases were withdrawn using syringe and needle sets, and were subsequently applied to LFA strips as described previously (see *3.2.7. Combining Concentration of M13 with the Lateral-Flow Immunoassay*). The results of the LFA with the prior concentration step are shown in Figure 3.2. While no test line appeared for the negative control solution, which did not contain any M13, the intensity of the test line decreased with the decreasing concentration of M13 until no test line appeared for the solution containing $1x10^{7}$ pfu/mL (Figure 3.2h). This indicated a detection limit of approximately $5x10^{7}$ pfu/mL for the M13 LFA when combined with the prior concentration step, which represented a 10-fold improvement of the detection limit of the LFA assay. Furthermore, the intensity of the test line for all the detectable concentrations clearly increased

when the concentration step was incorporated prior to the detection step. It should be noted that a volume ratio of only 1/9 was utilized as a proof-of-principle demonstration that the LFA's detection limit could be improved using the aqueous two-phase polymer-salt system. In the future, even lower volume ratios may be implemented or extractions-in-series may be used to yield greater concentration factors that can lead to even lower detection limits.

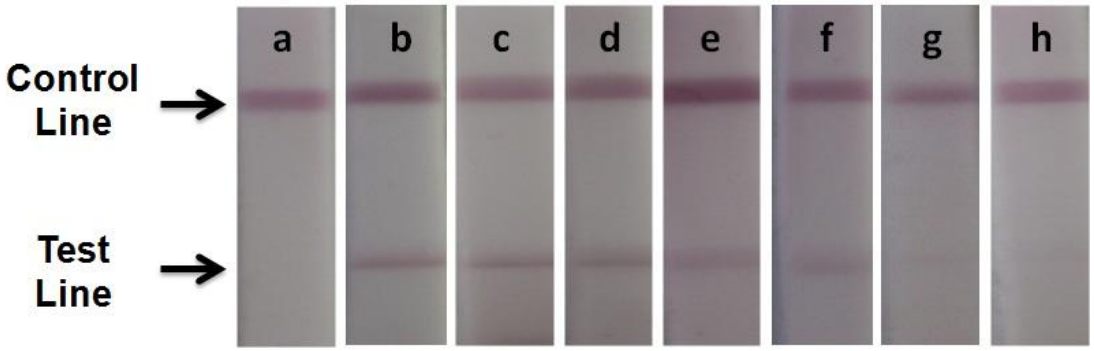

Figure 3.2. LFA used to detect bacteriophage M13 with the prior concentration step. The negative control without any M13 is shown in panel (a). The remaining solutions initially contained M13 at concentrations of (b) $1x10^{10}$, (c) $5x10^{9}$, (d) $1x10^{9}$, (e) $5x10^{8}$, (f) $1x10^{8}$, (g) $5x10^{7}$, and (h) $1x10^{7}$ pfu/mL.

3.4. Conclusions

Concentrating infectious agents, such as infectious viruses, prior to a detection step via LFA may improve the detection limit of the immunoassay, which in turn could significantly increase the effectiveness of using LFA for patient management at the POC. However, the concentration method must be implementable at the POC, meaning it must be able to utilize small sample volumes and require minimal training and power. Therefore, in this study, an aqueous two-phase polymer-salt system, which can be scalable for small sample volumes and designed to require minimal training and power, was investigated for concentrating a model virus, M13, prior to its detection via LFA. Furthermore, the aqueous two-phase polymer-salt system studied in this investigation is an improvement over the aqueous two-phase micellar

system previously studied by our research group [83] due to the faster phase separation time. The aqueous two-phase polymer-salt system was generated using PEG and potassium phosphate salt in phosphate-buffered saline. The partitioning behavior of M13 is expected to result from the hydrophilic nature of the outer viral coat and the repulsive, steric, excluded-volume interactions that operate between the polymer and M13 particles. The volume ratio was subsequently manipulated to concentrate M13 particles in the bottom, polymer-poor phase. For large partition coefficients, the concentration factor can be shown to depend on the volume ratio. At a volume ratio of 1/9, M13 particles were concentrated in the bottom phase by approximately 9 fold, matching closely with our predictions.

After demonstrating that we could concentrate M13 in the aqueous two-phase polymer-salt system in a predictive manner, we developed an LFA for the detection of M13 in-solution. The detection limit of the M13 LFA itself was found to be $5x10^8$ pfu/mL. M13 was subsequently concentrated approximately 10-fold by utilizing the aqueous two-phase polymer-salt system, which led to a 10-fold improvement in the LFA detection limit to $5x10^7$ pfu/mL. Therefore, we demonstrated that aqueous two-phase polymer-salt systems can be utilized to concentrate a target virus prior to the detection step. This was shown to improve the detection limit of the LFA and thereby increase the sensitivity of the immunoassay. This represents the first time that a fast phase separating aqueous two-phase system has been combined with LFA, and is an advance from our previous proof-of-concept study involving aqueous two-phase micellar systems. Furthermore, we show that when using alternative colloidal gold nanoparticles modified with a layer of PEG to provide stability in the high-salt containing solutions, the viability of the LFA is still maintained, and is a novel addition to the assay. In the future, higher concentration factors that yield even lower detection limits can be obtained through manipulating

operating conditions to obtain even lower volume ratios or performing extractions-in-series. We believe once optimized, the novel approach of utilizing aqueous two-phase systems to concentrate target biomolecules, such as infectious viruses, prior to the detection step could significantly improve the sensitivity of LFA. This in turn would enhance the LFA's effectiveness as a POC solution for preventing pandemic outbreaks, as well as for detecting biowarfare agents.

Chapter 4: Concluding Remarks

In this thesis, we have developed and demonstrated novel approaches for enhancing the lateral-flow immunoassay (LFA) detection of both proteins and viruses for applications in point-of-care diagnostics. This was accomplished by employing aqueous two-phase systems (ATPS) to concentrate the biomolecule target prior to its detection. In the first part of the thesis, we showed that small biomolecule targets, such as proteins, which partition evenly between the two-phases, could still be concentrated by employing colloidal gold nanoparticles to "fish" the target biomolecule into one of the two phases. A model protein, namely transferrin (Tf), was successfully concentrated using this method in an aqueous two-phase micellar system. Though this "fishing" approach was demonstrated using an aqueous two-phase micellar system, this method could be extended to other types of ATPS for concentrating small biomolecules. In the second part of the thesis, we successfully developed a method for concentrating a model virus, namely bacteriophage M13 (M13) in an aqueous two-phase polymer-salt system. This system, which phase separates on the order of minutes, is an improvement to our previous proof-of-principle study, which employed an aqueous two-phase micellar system that phase separates on the order of hours. This is a significant advance for the implementation of this technique geared towards improving detection and diagnostics in the point-of-care setting. In addition, we developed a new approach to the LFA test by modifying the colloidal gold nanoparticles to increase their stability in solutions of high-salt content. For both proteins and viruses, combining the concentration step with the LFA led to a 10-fold improvement of both detection limits. Table 4.1 below summarizes the novel developments and improvements to the capabilities of the biomolecule concentration method using the two ATPS that were investigated in this thesis.

Table 4.1. Summary of the novel developments and improvements to the capabilities of the biomolecule concentration method using ATPS.

ATPS	Constituents	Developed Capabilities	Phase separation time
Aqueous two-phase micellar system	Triton X-114 surfactant	"Fishing" with colloidal gold probes allows concentration of small biomolecules (<10 nm) such as proteins	18 hours
Aqueous two-phase polymer-salt system	PEG8000 polymer and Potassium-phosphate salt	Faster phase separation time is more appropriate for point-of-care diagnostics Modified gold-nanoparticles to achieve stability and prevent aggregation of the particles in high-salt solutions	< 30 minutes

Bibliography

1. Taylor, S.L. and S.L. Hefle, *Food allergen labeling in the USA and Europe.* Current opinion in allergy and clinical immunology, 2006. **6**(3): p. 186.

2. Schäppi, G.F., V. Konrad, D. Imhof, R. Etter, and B. Wüthrich, *Hidden peanut allergens detected in various foods: findings and legal measures.* Allergy, 2001. **56**(12): p. 1216-1220.

3. Broussard, L.A., *Biological agents: Weapons of warfare and bioterrorism.* Molecular Diagnosis, 2001. **6**(4): p. 323-333.

4. Ellison, D.H., *Handbook of chemical and biological warfare agents*. 2007: CRC.

5. Wong, R.C., H. Tse, and H.Y. Tse, *Lateral flow immunoassay*. 2008: Humana Pr Inc.

6. Shyu, R.H., H.F. Shyu, H.W. Liu, and S.S. Tang, *Colloidal gold-based immunochromatographic assay for detection of ricin.* Toxicon, 2002. **40**(3): p. 255-258.

7. Chiao, D.J., R.H. Shyu, C.S. Hu, H.Y. Chiang, and S.S. Tang, *Colloidal gold-based immunochromatographic assay for detection of botulinum neurotoxin type B.* J Chromatogr B Analyt Technol Biomed Life Sci, 2004. **809**(1): p. 37-41.

8. Schubert-Ullrich, P., J. Rudolf, P. Ansari, B. Galler, M. Führer, A. Molinelli, and S. Baumgartner, *Commercialized rapid immunoanalytical tests for determination of allergenic food proteins: an overview.* Analytical and Bioanalytical Chemistry, 2009. **395**(1): p. 69-81.

9. Peruski, A.H. and L.F. Peruski Jr, *Immunological methods for detection and identification of infectious disease and biological warfare agents.* Clinical and Vaccine Immunology, 2003. **10**(4): p. 506.

10. Wensing, M., A.H. Penninks, S.L. Hefle, S.J. Koppelman, C.A.F.M. Bruijnzeel-Koomen, and A.C. Knulst, *The distribution of individual threshold doses eliciting allergic reactions in a population with peanut allergy.* Journal of Allergy and Clinical Immunology, 2002. **110**(6): p. 915-920.

11. Ello-Martin, J.A., J.H. Ledikwe, and B.J. Rolls, *The influence of food portion size and energy density on energy intake: implications for weight management.* The American Journal of Clinical Nutrition, 2005. **82**(1): p. 236S-241S.

12. Ikeda, S., T. Kaneko, T. Okubo, L.E. Rallos, S. Eda, H. Mitsui, S. Sato, Y. Nakamura, S. Tabata, and K. Minamisawa, *Development of a bacterial cell enrichment method and its application to the community analysis in soybean stems.* Microb Ecol, 2009. **58**(4): p. 703-14.

13. *WHO Recommendations on the Use of Rapid Testing for Influenza Diagnosis*. 2005, World Health Organization.

14. Uyeki, T.M., R. Prasad, C. Vukotich, S. Stebbins, C.R. Rinaldo, Y. Ferng, S.S. Morse, E.L. Larson, A.E. Aiello, B. Davis, and A.S. Monto, *Low sensitivity of rapid diagnostic test for influenza.* Clinical Infectious Diseases, 2009. **48**(9): p. e89-e92.

15. Chanteau, S., L. Rahalison, M. Ratsitorahina, Mahafaly, M. Rasolomaharo, P. Boisier, T. O'Brien, J. Aldrich, A. Keleher, C. Morgan, and J. Burans, *Early diagnosis of bubonic plague using F1 antigen capture ELISA assay and rapid immunogold dipstick.* Int J Med Microbiol, 2000. **290**(3): p. 279-83.

16. Al-Yousif, Y., J. Anderson, C. Chard-Bergstrom, and S. Kapil, *Development, evaluation, and application of lateral-flow immunoassay (immunochromatography) for detection of rotavirus in bovine fecal samples.* Clinical and Vaccine Immunology, 2002. **9**(3): p. 723.

17. Laderman, E.I., E. Whitworth, E. Dumaual, M. Jones, A. Hudak, W. Hogrefe, J. Carney, and J. Groen, *Rapid, sensitive, and specific lateral-flow immunochromatographic point-of-care device for detection of herpes simplex virus type 2-specific immunoglobulin G antibodies in serum and whole blood.* Clinical and Vaccine Immunology, 2008. **15**(1): p. 159.

18. Cazacu, A.C., G.J. Demmler, M.A. Neuman, B.A. Forbes, S. Chung, J. Greer, A.E. Alvarez, R. Williams, and N.Y. Bartholoma, *Comparison of a new lateral-flow chromatographic membrane immunoassay to viral culture for rapid detection and differentiation of influenza A and B viruses in respiratory specimens.* Journal of clinical microbiology, 2004. **42**(8): p. 3661.

19. Nielsen, K., W.L. Yu, M. Lin, S.A.N. Davis, C. Elmgren, R. MacKenzie, J. Tanha, S. Li, G. Dubuc, and E.G. Brown, *Prototype single step lateral flow technology for detection of avian influenza virus and chicken antibody to avian influenza virus.* Journal of Immunoassay and Immunochemistry, 2007. **28**(4): p. 307-318.

20. Wong, R., *The effect of adulterants on urine screen for drugs of abuse: detection by an on-site dipstick device.* Am Clin Lab, 2002. **21**(1): p. 37-9.

21. Henderson, K. and J. Stewart, *A dipstick immunoassay to rapidly measure serum oestrone sulfate concentrations in horses.* Reprod Fertil Dev, 2000. **12**(3-4): p. 183-9.

22. Wittmann, C. and P.Y. Schreiter, *Analysis of terbuthylazine in soil samples by two test strip immunoassay formats using reflectance and luminescence detection.* J Agric Food Chem, 1999. **47**(7): p. 2733-7.

23. Cazacu, A.C., J. Greer, M. Taherivand, and G.J. Demmler, *Comparison of lateral-flow immunoassay and enzyme immunoassay with viral culture for rapid detection of influenza virus in nasal wash specimens from children.* Journal of Clinical Microbiology, 2003. **41**(5): p. 2132.

24. Gavin, P.J. and R.B. Thomson, *Review of Rapid Diagnostic Tests for Influenza.* Clinical and Applied Immunology Reviews, 2004. **4**(3): p. 151-172.

25. Ginocchio, C.C., F. Zhang, R. Manji, S. Arora, M. Bornfreund, L. Falk, M. Lotlikar, M. Kowerska, G. Becker, and D. Korologos, *Evaluation of multiple test methods for the detection of the novel 2009 influenza A (H1N1) during the New York City outbreak.* Journal of Clinical Virology, 2009. **45**(3): p. 191-195.

26. Uyeki, T.M., *Influenza diagnosis and treatment in children: a review of studies on clinically useful tests and antiviral treatment for influenza.* The Pediatric infectious disease journal, 2003. **22**(2): p. 164.

27. Faix, D.J., S.S. Sherman, and S.H. Waterman, *Rapid-test sensitivity for novel swine-origin influenza A (H1N1) virus in humans.* New England Journal of Medicine, 2009. **361**(7): p. 728.

28. Pritt, B. *Viral Culture Uses and Pitfalls*. 2012 May 31, 2012]; Available from: http://www.mayomedicallaboratories.com/mediax/articles/hottopic-pdfs/2012/2012-04-viral-culture-handout.pdf.

29. Elden, L.J.R.v., M.G.J.v. Kraaij, M. Nijhuis, K.A.W. Hendriksen, A.W. Dekker, M. Rozenberg-Arska, and A.M.v. Loon, *Polymerase Chain Reaction Is More Sensitive than Viral Culture and Antigen Testing for the Detection of Respiratory Viruses in Adults with Hematological Cancer and Pneumonia.* Clinical Infectious Diseases, 2002. **34**(2): p. 177-183.

30. Caram, L.B., J. Chen, E.W. Taggart, D.R. Hillyard, R. She, C.R. Polage, J. Twersky, K. Schmader, C.A. Petti, and C.W. Woods, *Respiratory Syncytial Virus Outbreak in a Long-Term Care Facility Detected Using Reverse Transcriptase Polymerase Chain Reaction: An Argument for Real-Time Detection Methods.* Journal of the American Geriatrics Society, 2009. **57**(3): p. 482-485.

31. McCabe, W.L., J.C. Smith, and P. Harriot, *Unit operations of chemical engineering*. 5 ed. 1993, New York: McGraw-Hill.

32. Albertsson, P., *Chromatography and partition of cells and cell fragments.* Nature, 1956. **177**: p. 771-774.

33. Albertsson, P., *Partition of proteins in liquid polymer-polymer two-phase systems.* Nature, 1958. **182**: p. 709-711.

34. Albertsson, P.A., *Partition of Cell Particles and Macromolecules*. 3 ed. 1986, New York: John Wiley & Sons.

35. Walter, H., D.E. Brooks, and D. Fisher, *Partitioning in aqueous two-phase systems: theory, methods, uses, and application to biotechnology*. 1985: Academic Pr.

36. Zaslavsky, B.Y., *Aqueous two-phase partitioning: physical chemistry and bioanalytical applications*. 1995: CRC.

37. Hatti-Kaul, R., *Aqueous two-phase systems.* Molecular Biotechnology, 2001. **19**(3): p. 269-277.

38. Quina, F.H. and W.L. Hinze, *Surfactant-Mediated Cloud Point Extractions: An Environmentally Benign Alternative Separation Approach.* Industrial & Engineering Chemistry Research, 1999. **38**(11): p. 4150 -4168.

39. Albertsson, P.A., *Separation of cells and cell organelles by partition in aqueous polymer two-phase systems.* Methods Enzymol, 1989. **171**: p. 532-49.

40. Albertsson, P.A., A. Cajarville, D.E. Brooks, and F. Tjerneld, *Partition of proteins in aqueous polymer two-phase systems and the effect of molecular weight of the polymer.* Biochim Biophys Acta, 1987. **926**(1): p. 87-93.

41. Capezio, L., D. Romanini, G.A. Pico, and B. Nerli, *Partition of whey milk proteins in aqueous two-phase systems of polyethylene glycol-phosphate as a starting point to isolate proteins expressed in transgenic milk.* J Chromatogr B Analyt Technol Biomed Life Sci, 2005. **819**(1): p. 25-31.

42. Elling, L., M.R. Kula, E. Hadas, and E. Katchalski-Katzir, *Partition of free and monoclonal-antibody-bound horseradish peroxidase in a two-phase aqueous polymer system--novel procedure for the determination of the apparent binding constant of monoclonal antibody to horseradish peroxidase.* Anal Biochem, 1991. **192**(1): p. 74-7.

43. Kamei, D.T., J.A. King, D.I. Wang, and D. Blankschtein, *Separating lysozyme from bacteriophage P22 in two-phase aqueous micellar systems.* Biotechnol Bioeng, 2002. **80**(2): p. 233-6.

44. Liu, C.L., D.T. Kamei, J.A. King, D.I. Wang, and D. Blankschtein, *Separation of proteins and viruses using two-phase aqueous micellar systems.* J Chromatogr B Biomed Sci Appl, 1998. **711**(1-2): p. 127-38.

45. Morre, D.M. and D.J. Morre, *Aqueous two-phase partition applied to the isolation of plasma membranes and Golgi apparatus from cultured mammalian cells.* J Chromatogr B Biomed Sci Appl, 2000. **743**(1-2): p. 377-87.

46. Rangel-Yagui, C.O., H. Lam, D.T. Kamei, D.I. Wang, A. Pessoa, Jr., and D. Blankschtein, *Glucose-6-phosphate dehydrogenase partitioning in two-phase aqueous mixed (nonionic/cationic) micellar systems.* Biotechnol Bioeng, 2003. **82**(4): p. 445-56.

47. Kresheck, G.C. and Z. Wang, *A new micellar aqueous two-phase partitioning system (ATPS) for the separation of proteins.* J Chromatogr B Analyt Technol Biomed Life Sci, 2007. **858**(1-2): p. 247-53.

48. Li, M. and T.L. Peeples, *Purification of hyperthermophilic archaeal amylolytic enzyme (MJA1) using thermoseparating aqueous two-phase systems.* J Chromatogr B Analyt Technol Biomed Life Sci, 2004. **807**(1): p. 69-74.

49. Rabelo, A.P., E.B. Tambourgi, and A. Pessoa, Jr., *Bromelain partitioning in two-phase aqueous systems containing PEO-PPO-PEO block copolymers.* J Chromatogr B Analyt Technol Biomed Life Sci, 2004. **807**(1): p. 61-8.

50. Kula, M.R., *Trends and future prospects of aqueous two-phase extraction.* Bioseparation, 1990. **1**(3-4): p. 181-9.

51. Johansson, H.O., G. Karlstrom, F. Tjerneld, and C.A. Haynes, *Driving forces for phase separation and partitioning in aqueous two-phase systems.* J Chromatogr B Biomed Sci Appl, 1998. **711**(1-2): p. 3-17.

52. Jyh-Ping, C., *Partitioning and separation of α-lactalbumin and β-lactoglobulin in PEG/potassium phosphate aqueous two-phase systems.* Journal of Fermentation and Bioengineering, 1992. **73**(2): p. 140-147.

53. Bordier, C., *Phase separation of integral membrane proteins in Triton X-114 solution.* J Biol Chem, 1981. **256**(4): p. 1604-7.

54. Nikas, Y.J., C.-L. Liu, T. Srivastava, N.L. Abbott, and D. Blankschtein, *Protein Partitioning in Two-Phase Aqueous Nonionic Micellar Solutions.* Macromolecules, 1992. **25**(18): p. 4797-4806.

55. Lue, L. and D. Blankschtein, *A Liquid-State Theory Approach to Modeling Solute Partitioning in Phase-Separated Solutions.* Industrial & Engineering Chemistry Research, 1996. **35**(9): p. 3032 -3043.

56. Israelachvili, J.N., *Intermolecular and surface forces*. 2 ed. 1992, San Diego, CA: Academic Press.

57. Tanford, C., *The hydrophobic effect: Formation of micelles and biological membranes, p1-10*. 2 ed. 1978, New York: John Wiley & Sons.

58. Mashayekhi, F., A.S. Meyer, S.A. Shiigi, V. Nguyen, and D.T. Kamei, *Concentration of mammalian genomic DNA using two-phase aqueous micellar systems.* Biotechnol Bioeng, 2009. **102**(6): p. 1613-23.

59. Kamei, D.T., C.L. Liu, C. Haase-Pettingell, J.A. King, D.I. Wang, and D. Blankschtein, *Understanding viral partitioning in two-phase aqueous nonionic micellar systems: 1. Role of attractive interactions between viruses and micelles.* Biotechnol Bioeng, 2002. **78**(2): p. 190-202.

60. Kamei, D.T., D.I.C. Wang, and D. Blankschtein, *Fundamental Investigation of Protein Partitioning in Two-Phase Aqueous Mixed (Nonionic/Ionic) Micellar Systems.* Langmuir, 2002. **18**(8): p. 3047-3057.

61. Huddleston, J., A. Veide, K. Kohler, J. Flanagan, S.O. Enfors, and A. Lyddiatt, *The molecular basis of partitioning in aqueous two-phase systems.* Trends in Biotechnology, 1991. **9**(11): p. 381-8.

62. Gupta, V., S. Nath, and S. Chand, *Role of water structure on phase separation in polyelectrolyte–polyethyleneglycol based aqueous two-phase systems.* Polymer, 2002. **43**(11): p. 3387-3390.

63. Zaslavsky, B.Y., *Bioanalytical applications of partitioning in aqueous polymer two-phase systems.* Analytical Chemistry, 1992. **64**(15): p. 765A-773A.

64. Shuval, H.I., B.F.S. Cymbalista, and N. Goldblum, *The phase-separation method for the concentration and detection of viruses in water.* Water Research, 1969. **3**(4): p. 225-240.

65. Hammar, L., *Concentration and Purification of Viruses Aqueous Two-Phase Systems: Methods and Protocols*, R. Hatti-Kaul, Editor. 2000, Humana Press. p. 143-158.

66. Gomes, G.A., A.M. Azevedo, M.R. Aires-Barros, and D.M.F. Prazeres, *Purification of plasmid DNA with aqueous two phase systems of PEG 600 and sodium citrate/ammonium sulfate.* Separation and Purification Technology, 2009. **65**(1): p. 22-30.

67. Spruijt, R.B., A.B. Meijer, C.J. Wolfs, and M.A. Hemminga, *Localization and rearrangement modulation of the N-terminal arm of the membrane-bound major coat protein of bacteriophage M13.* Biochimica et Biophysica Acta, 2000. **1509**(1-2): p. 311-23.

68. Wong, R.C. and H.Y. Tse, *Lateral flow immunoassay*: Springer.

69. Posthuma-Trumpie, G.A., J. Korf, and A. van Amerongen, *Lateral flow (immuno) assay: its strengths, weaknesses, opportunities and threats. A literature survey.* Analytical and Bioanalytical Chemistry, 2009. **393**(2): p. 569-582.

70. Chen, R., T.M. Li, H. Merrick, R.F. Parrish, V. Bruno, A. Kwong, C. Stiso, and D.J. Litman, *An internal clock reaction used in a one-step enzyme immunochromatographic assay of theophylline in whole blood.* Clin Chem, 1987. **33**(9): p. 1521-5.

71. Ribeiro, S.C., G.A. Monteiro, J.M. Cabral, and D.M. Prazeres, *Isolation of plasmid DNA from cell lysates by aqueous two-phase systems.* Biotechnol Bioeng, 2002. **78**(4): p. 376-84.

72. Mashayekhi, F., R. Chiu, A. Le, F. Chao, B. Wu, and D. Kamei, *Enhancing the lateral-flow immunoassay for viral detection using an aqueous two-phase micellar system.* Analytical and Bioanalytical Chemistry, 2010. **398**(7): p. 2955-2961.

73. Frens, G., *Particle size and sol stability in metal colloids.* Colloid & Polymer Science, 1972. **250**(7): p. 736-741.

74. Horisberger, M. and M.F. Clerc, *Labelling of colloidal gold with protein A. A quantitative study.* Histochemistry, 1985. **82**(3): p. 219-23.

75. Leuvering, J.H., P.J. Thal, M. van der Waart, and A.H. Schuurs, *Sol particle immunoassay (SPIA).* J Immunoassay, 1980. **1**(1): p. 77-91.

76. Kamei, D.T., J.A. King, D.I. Wang, and D. Blankschtein, *Understanding viral partitioning in two-phase aqueous nonionic micellar systems: 2. Effect of entrained micelle-poor domains.* Biotechnol Bioeng, 2002. **78**(2): p. 203-16.

77. Christopher, P., N. Robinson, and M.K. Shaw, *Antibody-label conjugates in lateral-flow assays.* Drugs of Abuse, 2005: p. 87-98.

78. Albertsson, P.A., *Partition of cell particles and macromolecules in polymer two-phase systems.* Adv Protein Chem, 1970. **24**: p. 309-341.

79. Mashayekhi, F., R.Y. Chiu, A.M. Le, F.C. Chao, B.M. Wu, and D.T. Kamei, *Enhancing the lateral-flow immunoassay for viral detection using an aqueous two-phase micellar system.* Anal Bioanal Chem, 2010.

80. Chun, P., *Colloidal Gold and Other Labels for Lateral Flow Immunoassays Lateral Flow Immunoassay*, R. Wong and H. Tse, Editors. 2009, Humana Press. p. 1-19.

81. Carlson, K., *Appendix: working with bacteriophages: common techniques and methodological approaches*, in *Bacteriophages: Biology and applications*, E. Kutter and A. Sulakvelidze, Editors. 2005, CRC Press Boca Raton, FL. p. 437–494.

82. Haiss, W., N.T. Thanh, J. Aveyard, and D.G. Fernig, *Determination of size and concentration of gold nanoparticles from UV-vis spectra.* Analytical Chemistry, 2007. **79**(11): p. 4215-21.

83. Mashayekhi, F., R.Y. Chiu, A.M. Le, F.C. Chao, B.M. Wu, and D.T. Kamei, *Enhancing the lateral-flow immunoassay for viral detection using an aqueous two-phase micellar system.* Analytical and Bioanalytical Chemistry, 2010. **398**(7-8): p. 2955-61.